

## Slope selection in unstable multilayer growth in 1 + 1 dimensions: Step flow models with downward funneling

Ian Johnson <sup>\*</sup>

*Department of Mathematics, University of Maryland, College Park, Maryland 20742, USA*

Christian Ratsch <sup>†</sup>

*Institute for Pure and Applied Mathematics and Department of Mathematics, University of California, Los Angeles, California 90095, USA*

Frederic Gibou <sup>‡</sup>

*Department of Mechanical Engineering, Department of Computer Science, and Department of Mathematics, University of California, Santa Barbara, California 93106, USA*

Dionisios Margetis <sup>§</sup>

*Institute for Physical Science and Technology, Department of Mathematics, and Center for Scientific Computation and Mathematical Modeling, University of Maryland, College Park, Maryland 20742, USA*



(Received 10 July 2019; published 18 November 2019)

We study analytically and numerically aspects of the dynamics of slope selection for one-dimensional models describing the motion of line defects, steps, in homoepitaxial crystal growth. The kinetic processes include diffusion of adsorbed atoms (adatoms) on terraces, attachment and detachment of atoms at steps with large yet finite, positive Ehrlich-Schwoebel step-edge barriers, material deposition on the surface from above, and the mechanism of downward funneling (DF) via a phenomenological parameter. In this context, we account for the influence of boundary conditions at extremal steps on the dynamics of slope selection. Furthermore, we consider the effect of repulsive, nearest-neighbor force-dipole step-step interactions. For geometries with straight steps, we carry out numerical simulations of step flow, which demonstrate that slope selection eventually occurs. We apply perturbation theory to characterize time-periodic solutions of step flow for slope-selected profiles. By this method, we show how a simplified step flow theory with constant probabilities for the motion of deposited atoms can serve as an effective model of slope selection in the presence of DF. Our analytical findings compare favorably to step simulations.

DOI: [10.1103/PhysRevE.100.052802](https://doi.org/10.1103/PhysRevE.100.052802)

### I. INTRODUCTION

Epitaxial growth comprises kinetic processes and thermodynamic effects that contribute to the formation and evolution of thin films and nanostructures on crystal surfaces. To predict the evolving crystal surface morphology under growth conditions, it is imperative to develop reliable models for the underlying out-of-equilibrium dynamics, from the atomistic scale to the continuum [1,2]. This goal gives rise to a hierarchy of kinetic models, which include atomistic descriptions such as kinetic Monte Carlo (KMC) algorithms, mesoscale theories which aim to capture the motion of line defects (steps) at the nanoscale [3,4], and continuum models which may emerge from the coarse graining of individual atoms or atomic layers at larger scales [5–7].

In homoepitaxial growth, in particular, the material deposited on the surface takes on the crystalline orientation of the substrate. An aspect of homoepitaxy that has been

the subject of intensive studies is the evolution of mounds during unstable growth. In situations of experimental interest, islands successively nucleate on top of other islands and can ultimately form a crystalline mound. It is well known that this surface instability is driven by kinetic mechanisms such as the Ehrlich-Schwoebel (ES) effect, which signifies the energy barrier inhibiting transport of adsorbed atoms (adatoms) between atomic layers [4,8,9].

With this paper, our goal is to describe how kinetic and thermodynamic ingredients of step flow may affect the long-time surface profiles in slope selection. We use a step flow model with an ad hoc *downward funneling* (DF) mechanism, by which atoms landing on the surface from above are incorporated to the lower step edge and, thus, create a lateral *downhill* current that favors slope selection [10–12]. In our formulation, the DF mechanism is assumed to be present, and is introduced into the model through a phenomenological parameter. This modeling of DF is adopted from Refs. [13–16], but is combined with additional step flow ingredients. We observe and study the dynamical appearance of slope selection numerically. By assuming that slope selection ultimately occurs, we analytically describe properties of the final slope selected profile.

<sup>\*</sup>fourfouriers@gmail.com

<sup>†</sup>cratsch@ipam.ucla.edu

<sup>‡</sup>fgibou@ucsb.edu

<sup>§</sup>dio@math.umd.edu

The DF mechanism has been the subject of a series of investigations, which usually (albeit not always) invoke KMC simulations or continuum models. Here, we adopt a mesoscale perspective. By using a perturbation technique for step flow equations, we analyze the joint effect on slope-selected profiles of the following mechanisms: DF, finite but large ES barriers, and force-dipole step-step interactions in one spatial dimension (1D), when the step edges are straight. In our analysis, we use a semi-infinite step train.

Before we proceed to the specifics of our approach, let us review slope selection and the DF mechanism in homoepitaxial growth. First, consider the effect of the ES barrier in the absence of DF. In principle, the ES barrier can reduce the likelihood that an atom deposited on an island will move to the lower layer (step) and attach to the same island. This effect alone would result in a lateral uphill current on the growing mound. This current can in turn cause accumulation of material near the top of the mound, thus facilitating the nucleation of islands. Consequently, at long enough times, the surface as a whole would coarsen as neighboring islands would encroach upon one another. If this phenomenon occurred, the lower islands would grow more slowly. As a result, the boundaries between islands, which are steps, would bunch together. Hence, the mound would become progressively more steep, eventually forming a single large step bunch, with an interstep spacing comparable to the size of a critical nucleus. Such a steepening process may also be driven by effects other than an ES barrier, e.g., long-range attractive step-step interactions [17].

However, experimental observations have indicated that the spacing between steps in growing mounds often remains significantly larger than the radius of the critical nucleus, even when the ES barrier is large compared to the Boltzmann energy,  $k_B T$ ; see, e.g., Refs. [18–20]. These observations suggest that there exists a downhill current that causes the mound slope to stabilize over time and eventually tends to slightly fluctuate around an equilibrium value. This stabilization signifies slope selection. To account systematically for the requisite downhill current, one can explicitly add a corresponding kinetic mechanism such as DF to models of surface dynamics at the atomistic, mesoscopic, or macroscopic scale. Our work here elaborates on aspects of this theme by exploiting the dynamical character of step flow models.

We remark that although slope selection critically depends on a kinetic mechanism for downhill current, the origin of this current is not necessarily DF. For example, it has been shown that a combination of short-range attractive step-step interactions and long-range repulsive step-step interactions may drive a relaxing vicinal surface toward forming an array of step bunches [21,22]. In this situation, the step spacing and number of steps in each bunch is determined by the relative strengths of the two types of interactions. This behavior within a bunch may be recognized as a form of slope selection, caused by the balance between attractive forces between steps within a bunch and repulsive forces between distinct bunches.

A close look at the existing, extensive literature on slope selection indicates the variety of models, approaches, and results. It is impossible to exhaustively list the related bibliography here. A significant portion of these works seeks atomistic descriptions of the system via KMC simulations, by which the atom hopping on the crystal surface is

suitably modeled so as to kinetically favor a downhill current on mounds [10,13,23,24]. Some of these works invoke an atomistic model with a transient mobility with a search region whose linear size is prescribed as an input parameter of the KMC simulations (see, e.g., the broad review in Ref. [25]). In juxtaposition to this approach, one should place phenomenological continuum-scale models for slope selection, which rely on the use of fourth- or sixth-order partial differential equations for the evolving surface height; see, e.g., [26–31]. These evolution equations usually have the structure of gradient descent of a slope-dependent energy, and allow for slope selection via coarsening dynamics. Computations by use of KMC simulations and continuum theories for mounds lie beyond our present scope.

A third, less developed approach to slope selection invokes the motion of steps [13–16]. In this view, the slope is determined by the widths of terraces that bound steps, and slope selection means that these widths asymptotically approach certain values. Generally speaking, the main ingredients of step flow models are [3,32] (i) a step velocity law through mass conservation, (ii) the diffusion of adatoms on terraces between steps, and (iii) the attachment and detachment of atoms at steps, expressed by suitable boundary conditions for the adatom density at step edges. Furthermore, the elastic force-dipole step-step interactions can in principle be incorporated into the underlying step energy [33,34]. This framework is mesoscopic in the sense that it retains features of both the atomistic and the continuum scale: the diffusion of adatoms in the lateral direction is continuous yet atomistic discreteness is kept in the vertical direction. The kinetic parameters of step flow depend on energy barriers in correspondence to atomistic dynamics.

In this paper, we use a step flow model with DF in order to analyze dynamical aspects of slope selection in 1D. We choose to incorporate DF in step flow via a phenomenological parameter, the prescribed length  $L_{DF}$ , in the spirit of Refs. [13–16]. From an atomistic view,  $L_{DF}$  plausibly measures the order of magnitude of the linear size of the search region used in KMC simulations with a transient mobility, along the lines discussed in [25]. However, there is no derivation of this form of the DF mechanism in the mesoscale picture from atomistic dynamics at this point.

In our step flow model, the DF mechanism modifies the usual diffusion process of adatoms through the requirement that deposition on the surface from above occurs nonuniformly on each terrace: atoms that would otherwise be deposited from above on the upper terrace and close enough to a step edge are now directly incorporated into the lower step edge (rather than allowed to land on the upper terrace). This effect results in a downward mass current. In our formulation, the basic ingredients of step motion, namely, mass conservation, terrace diffusion, and attachment and detachment, remain essentially intact. In addition, our model accounts for nearest-neighbor, force-dipole step-step interactions. Most importantly, we also include the creation and annihilation of *extremal steps* via respective boundary conditions. These small-scale events driven by the assumed DF (through the parameter  $L_{DF}$ ) form a key ingredient of our formulation, since they lead to slope selection at the macroscopic scale. This slope selection is verified by our numerics.

Our approach results in a nonlinear system of ordinary differential equations (ODEs) for the step positions, which are subject to the step creation and annihilation conditions mentioned above. The dynamical properties of the respective solutions are the focus of our investigation. To enable tangible predictions without losing sight of the key physical mechanisms, we apply perturbation theory by treating nonlinearities in these ODEs as sufficiently small. In this vein, we properly derive and solve a linear system which provides the zeroth-order solution of our perturbative scheme, expecting that corrections are sufficiently small. This view turns out to be compatible with our step simulations.

It is worthwhile to compare this mesoscale description to other works in slope selection, in an effort to further motivate our present choice of models. We note a few major advantages of the mesoscale perspective, beginning with macroscale models. In our physical setting, perhaps the most important advantage is the ability to explicitly incorporate discrete dynamical processes, including step annihilations and creations. Such processes can in principle be included in a macroscale model, but in practice they are often neglected or suppressed, for example by using periodic boundary conditions (e.g., Refs. [30,31]). In the present paper, we show that such processes can be key ingredients of slope selection. In particular, if we modify our model *only* by removing all special behavior at extremal steps, we find that no particular slope is selected; instead, all surface profiles with constant terrace widths are steady states.

We can point to advantages of our approach in comparison to atomistic models as well. As we see in this paper, the use of a mesoscale model allows us to obtain analytical insight through perturbative techniques. In addition, the combination of DF with elastic force-dipole step-step interactions is absent in past works, despite the fact that the latter are expected to be present in a wide variety of physical settings. Hence, our work forms an extension of the interaction-free step flow models formulated in Refs. [13–16]. We venture to add that it is in principle computationally demanding to include the effect of elastic interactions in KMC simulations.

In a more technical language, in this paper we explicitly characterize the *saturation surface profile* a la Schinzer [13]. This profile expresses a configuration of step positions that is reproduced upon deposition of one monolayer (ML) of atoms. Aspects of the dynamics of the saturation profile are also studied in Refs. [14–16]. In these works, the analysis addresses the somewhat idealized case in which the ES barrier is infinite, and step-step interactions are absent. Here, we aim to extend these results to the case where the ES barrier is large but *finite*, and step-step interactions influence the equilibrium adatom density at step edges. A distinctive ingredient of our analysis is the use of perturbations to extract an approximate solution to a system of equations that demonstrate *weak nonlinear couplings*. We explicitly solve a truncated hierarchy of the resulting linear equations for a semi-infinite step train. The underlying notion of perturbation will be made precise in our analysis.

We start from an idealized, linear step flow model that uses constant probabilities for any atom deposited on a terrace to move to the lower or upper step edge. Then, we analyze a nonlinear step model with irreversible growth, i.e., when the equilibrium density of adatoms at the step edges is negligibly

small. Notably, we analytically demonstrate in what sense the former, simplified model can be viewed as an *effective theory* for the latter model in the kinetic regime of a sufficiently small DF effect.

Our approach leaves a few open questions. For instance, since we make use of a semi-infinite 1D mound in our analysis, we fail to include any explicit condition for the nucleation of atomic layers. This choice is considered as physically reasonable given the dimensionality of the problem. Even in a 1D finite mound (which is considered, e.g., in Refs. [14–16], and used in our step simulations here), one cannot formulate *realistic* conditions for nucleation of atomic layers. In a similar vein, we do not address the computations of roughening and coarsening exponents that characterize epitaxial growth in the presence of DF. (Recently, this aspect was reexamined via KMC simulations [25].) Although our goal is to describe a dynamical steady state, we leave unexplored any questions about the transient dynamics leading to this state. The issue of transient dynamics is closely related to the aforementioned question about nucleation, because the approach of a system to a steady state in the present setting with a mound in homoepitaxy is driven by the competition between the creation and annihilation of steps.

The remainder of the paper is organized as follows. In Sec. II, we formulate the relevant step flow models. In Sec. III, we consider a simplified version of the step flow model involving constant probabilities for atom kinetics, and extract information about the saturation profile by using perturbation theory. Our analysis partly makes use of the method of generating function in order to solve the (discrete) difference scheme for step positions. In Sec. IV, we treat irreversible growth by constructing a perturbative hierarchy and compare the results to step simulations. In Sec. V, we study the reversible case of the step flow model by including the joint effect of DF and step-step interactions. In Sec. VI, we discuss closely related problems such as the setting of radial geometry and aspects of a fully continuum theory. Finally, Sec. VII concludes our paper with an overview of the results.

## II. 1D STEP FLOW MODEL: FORMULATION

In this section, we review the basic elements of step flow which permeate the Burton, Cabrera, and Frank (BCF) model [32]. Furthermore, we describe an extension of this model that directly incorporates the DF mechanism [14–16,35]. The geometry consists of a monotone step train with ascending steps of atomic height  $a$  in the  $x$  direction, as shown in Fig. 1. (A similar figure appears in [14]; see their Fig. 1.) The steps have positions  $x_n$  with  $x_0 = 0$ , and the  $n$ th terrace is the region defined by  $x_n < x < x_{n+1}$ . The step positions are time dependent, viz.,  $x_n = x_n(t)$ , with prescribed initial values  $x_n(0)$  ( $t \geq 0$ ). The steps are considered to advance when they move from right to left and retreat otherwise (see Fig. 1). In our analysis, we consider a semi-infinite step train, where  $n = 0, 1, \dots$ . Note, however, that in our step simulations (Sec. IV C), the step train is taken to be finite.

### A. Diffusion processes and step-step interactions

An ingredient of the BCF model is the continuous diffusion of adatoms. Let  $c_n(x, t)$  denote the density of adatoms in the

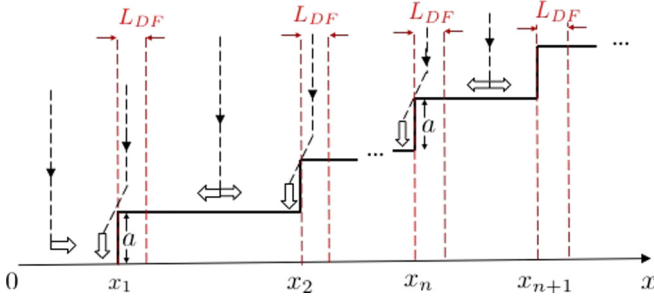


FIG. 1. Schematic of step geometry with DF [14]. The  $n$ th step has microscale height  $a$  and position  $x_n$  with  $x_0 = 0$ , and the  $n$ th terrace is the region  $x_n < x < x_{n+1}$  ( $n = 0, 1, \dots$ ). Each pair of red, vertical, dashed lines indicates the DF-affected part, of length  $L_{DF}$ , for every terrace. Dashed crooked lines ending in wide arrows indicate adatom attachment by DF. Dashed straight lines ending in pairs of arrows indicate terrace diffusion. Atoms deposited onto the bottom terrace ( $0 < x < x_1$ ) diffuse to the right, toward the (ascending) step at  $x = x_1$ .

$n$ th terrace. This  $c_n(x, t)$  satisfies the equation

$$\frac{\partial c_n}{\partial t} = F + D \frac{\partial^2 c_n}{\partial x^2} - \tau^{-1} c_n, \quad x_n < x < x_{n+1}, \quad (1)$$

where  $D$  is the terrace diffusivity,  $F$  expresses the deposition flux, and  $\tau^{-1}$  is the evaporation rate. We assume that  $F$  is a constant. To simplify the analysis, we neglect evaporation, thus setting  $\tau^{-1} c_n = 0$ .

Second, Eq. (1) needs boundary conditions which account for the attachment and detachment of atoms at step edges. These processes are modeled by the kinetic relation [36,37]

$$\begin{aligned} \pm \frac{\partial c_j}{\partial x} \Big|_{x=x_n^\pm} &= \frac{1}{L_\mp} [c_j(x_n^\pm, t) - c_n^{\text{eq}}] \\ &\pm \frac{1}{L_p} [c_n(x_n^+, t) - c_{n-1}(x_n^-, t)], \end{aligned} \quad (2)$$

on the right (+), with  $j = n$ , or left (-), with  $j = n - 1$ , of the  $n$ th step (see Fig. 1). Here, we define the length  $L_\pm = D/k_\pm$  where  $k_\pm$  are kinetic parameters for the exchange of atoms with the ascending (+) or descending (-) step, according to the ES effect [8,9]; for a positive ES barrier, we have  $k_+ > k_-$  and, thus,  $L_+ < L_-$ . Analogously, we define the length  $L_p = D/k_p$  where  $k_p$  is a kinetic parameter for step permeability; by this mechanism, atoms can hop directly over the step from one terrace to another [37]. Finally,  $c_n^{\text{eq}}$  is the equilibrium adatom density at the  $n$ th step. Note that when attachment is irreversible, we have  $c_n^{\text{eq}} \simeq 0$ ; by slightly abusing terminology, we will occasionally refer to this situation as irreversible step flow. Within the present study, we neglect step permeability, taking  $L_p \rightarrow \infty$ .

Equations (1) and (2) must be supplemented with the step velocity law. Mass conservation dictates that

$$\frac{dx_n}{dt} = -Da \left( \frac{\partial c_n}{\partial x} - \frac{\partial c_{n-1}}{\partial x} \right) \Big|_{x=x_n}, \quad (3)$$

where  $-D(\partial c_n/\partial x)$  is the adatom flux on the  $n$ th terrace and  $a$  is the lattice spacing. In Eq. (3),  $\partial c_n/\partial x$  is evaluated on the

right ( $x = x_n^+$ ) and  $\partial c_{n-1}/\partial x$  is evaluated on the left ( $x = x_n^-$ ) of the  $n$ th step.

It remains to describe the equilibrium adatom concentration,  $c_n^{\text{eq}}$ , at the  $n$ th step; cf. Eq. (2). This quantity may in principle account for thermodynamic effects in the step configuration, including elastic force-dipole as well as entropic step-step interactions. Such effects are captured by the total step energy,  $E_{\text{st}}$ , which depends on the step positions,  $x_n$ . By invoking the Gibbs-Thomson relation [3], we write

$$c_n^{\text{eq}} = c^{\text{eq}} \exp\left(\frac{\mu_n}{k_B T}\right). \quad (4a)$$

In the above,  $\mu_n$  is the  $n$ th step chemical potential, a thermodynamic force given by the variation of  $E_{\text{st}}$  [2,3], viz.,

$$\mu_n = -\frac{\partial E_{\text{st}}}{\partial x_n} \quad (\text{for fixed } t > 0). \quad (4b)$$

By invoking a widely used model for energy functional  $E_{\text{st}}(\{x_n\}_{n \geq 0})$  [2,3], we take

$$E_{\text{st}} = g \sum_n (x_{n+1} - x_n)^{-2}, \quad (4c)$$

where  $g$  is the interaction strength. Notably, Eq. (4c) accounts for entropic and force-dipole elastic step-step interactions in 1D. By considering these interactions as repulsive, we assume  $g > 0$ . The parameter  $g$  is computed to be [3]

$$g = \frac{(\pi k_B T)^2}{24a^3 \tilde{\beta}} \left[ 1 + \sqrt{1 + \frac{4A\tilde{\beta}}{(k_B T)^2}} \right]^2,$$

where  $\tilde{\beta}$  is the step stiffness and  $A$  expresses the purely elastic contribution to the energy of a single step. Equation (4c) can be modified to include long-range elastic step interactions as well as interactions mediated by electronic surface states. Such extensions for  $E_{\text{st}}$  lie beyond our present scope.

## B. Modifications: DF and step annihilation

Next, we incorporate DF into the nanoscale step model.

### 1. Diffusion with DF on terraces

By the DF mechanism, atoms deposited from above onto the region  $x_n < x < x_n + L_{DF}$  of the  $n$ th terrace are funneled downward and are directly incorporated into the step edge, at  $x = x_n$ , instead of diffusing on the surface; see Fig. 1. The length scale,  $L_{DF}$ , for this process is introduced phenomenologically [13–16].

The diffusion equation takes the form (with  $\tau^{-1} c_n = 0$ )

$$\frac{\partial c_n}{\partial t} = F_n(x) + D \frac{\partial^2 c_n}{\partial x^2}, \quad (5a)$$

where

$$F_n(x) = \begin{cases} F, & \text{if } x_n + L_{DF} < x < x_{n+1}, \\ 0, & \text{if } x_n < x < x_n + L_{DF}. \end{cases} \quad (5b)$$

This modification is included only for  $n > 0$ . No DF occurs from the bottom terrace. Thus, the diffusion equation for  $c_0$  is left unaltered; cf. Eq. (1) with  $\tau^{-1} c_0 = 0$ . Additionally, the top terrace has the right end point  $x = L_{\text{tot}}$ , which forms the right end point of the domain because the top terrace has

no ascending step. This point  $x = L_{\text{tot}}$  is given by the initial condition, and it remains intact by the dynamics.

Taking into account mass conservation, the (modified) velocity law for the  $n$ th step reads

$$\frac{dx_n}{dt} = -Da \left( \frac{\partial c_n}{\partial x} - \frac{\partial c_{n-1}}{\partial x} \right) \Big|_{x=x_n} - FaL_{\text{DF}}. \quad (6)$$

Note that boundary condition (2) provides the requisite fluxes  $\frac{\partial c_n}{\partial x}$  at all boundaries except for  $x = 0$  and  $x = L_{\text{tot}}$  (which are not step edges). At each of these boundaries, we impose a no-flux condition, viz.,

$$\frac{\partial c_0}{\partial x} \Big|_{x=0} = 0, \quad \frac{\partial c_N}{\partial x} \Big|_{x=L_{\text{tot}}} = 0.$$

Because the deposition (source) terms  $F_n(x)$  have jump discontinuities, we also need to impose boundary conditions at the points  $\bar{x}_n = x_n + L_{\text{DF}}$ , inside each terrace ( $n = 1, 2, \dots$ ); cf. Fig. 1. These conditions dictate the continuity of the adatom density and flux at the point  $\bar{x}_n$ , viz.,

$$c_n(\bar{x}_n^-) = c_n(\bar{x}_n^+), \quad (7a)$$

$$\frac{\partial c_n}{\partial x} \Big|_{\bar{x}_n^-} = \frac{\partial c_n}{\partial x} \Big|_{\bar{x}_n^+}. \quad (7b)$$

By these conditions, adatoms do not accumulate at  $\bar{x}_n$ .

## 2. Explicit step velocity law with DF

Next, we use the solution of diffusion equation (5) to describe in some detail the velocity,  $dx_n/dt$ , of the  $n$ th step. First, we apply the quasistatic approximation, by which

$$\frac{\partial c_n}{\partial t} \approx 0,$$

in all terraces ( $n = 0, 1, \dots$ ). Thus, the adatom diffusion equation can be solved explicitly on each terrace in simple form.

Consequently, step velocity law (6) is written as

$$\frac{dx_n}{dt} = -a(J_n^{\text{dep}} + J_n^{\text{int}}). \quad (8a)$$

In the above,  $J_n^{\text{dep}}$  and  $J_n^{\text{int}}$  denote the mass fluxes due to the external material deposition and the differences in the chemical potentials of neighboring steps, respectively. For all steps other than the bottom step  $x_1$  and the top step  $x_N$ , we have

$$J_n^{\text{int}} = D \frac{c_{n+1}^{\text{eq}} - c_n^{\text{eq}}}{(x_{n+1} - x_n) + L_+ + L_-} + D \frac{c_{n-1}^{\text{eq}} - c_n^{\text{eq}}}{(x_n - x_{n-1}) + L_+ + L_-}, \quad (8b)$$

$$J_n^{\text{dep}} = FL_{\text{DF}} + \frac{F}{2} \left( 1 + \frac{L_- - L_+ + L_{\text{DF}}}{L_+ + L_- + x_n - x_{n-1}} \right) \times (x_n - x_{n-1} - L_{\text{DF}}) + \frac{F}{2} \left( 1 - \frac{L_- - L_+ + L_{\text{DF}}}{L_+ + L_- + x_{n+1} - x_n} \right) \times (x_{n+1} - x_n - L_{\text{DF}}). \quad (8c)$$

Recall that  $L_{\pm} = D/k_{\pm}$  where  $k_{\pm}$  are kinetic rates for the atom detachment (+) or attachment (−) at each step edge [8,9]. On

the bottom terrace, the absence of a lower terrace and the no-flux condition at  $x = 0$  result in

$$J_1^{\text{int}} = D \frac{c_2^{\text{eq}} - c_1^{\text{eq}}}{(x_2 - x_1) + L_+ + L_-}, \quad (8d)$$

$$J_1^{\text{dep}} = FL_{\text{DF}} + Fx_1 + \frac{F}{2} \left( 1 - \frac{L_- - L_+ + L_{\text{DF}}}{L_+ + L_- + x_2 - x_1} \right) \times (x_2 - x_1 - L_{\text{DF}}). \quad (8e)$$

On the top terrace, the no-flux condition at  $x = L_{\text{tot}}$  implies

$$J_N^{\text{int}} = D \frac{c_{N-1}^{\text{eq}} - c_N^{\text{eq}}}{(x_N - x_{N-1}) + L_+ + L_-} \quad (8f)$$

while  $J_N^{\text{dep}}$  takes the form of Eq. (8c), with  $x_{n+1}$  replaced by  $L_{\text{tot}}$ . Notably, the sum of the deposition fluxes,  $J_n^{\text{dep}}$ , is not equal to the total deposition flux,  $FL_{\text{tot}}$ . The difference between these two quantities is incorporated into the step creation condition; see Sec. II B 3.

Before proceeding, we point out that large yet finite, positive ES barriers [8,9] are of particular interest in our treatment; i.e., we assume that  $k_+ \gg k_-$ . Accordingly, to simplify the analysis slightly, we introduce the ES length as

$$L_{\text{ES}} = L_- - L_+ = \frac{D}{k_-} - \frac{D}{k_+},$$

and then neglect  $L_+$ ; thus,  $L_{\text{ES}} \simeq L_-$  [38]. The treatment of  $L_+$  as negligibly small is not essential, but simplifies the model without loss of the key physics of DF in our setting.

## 3. Step annihilation and creation

Next, we incorporate the step annihilation and creation conditions. In the former case, the main idea is to remove the bottom step, at  $x = x_1$ , from the system when this step reaches the origin,  $x = 0$ . Explicitly, we introduce the step annihilation times  $t_i$  ( $i = 1, 2, \dots$ ) by the property

$$\lim_{t \rightarrow t_i^-} x_1(t) = 0. \quad (9a)$$

At these times we impose

$$x_n(t_i) = \lim_{t \rightarrow t_i^-} x_{n+1}(t). \quad (9b)$$

Physically, Eq. (9b) may be understood from the point of view of coarsening of a large number of two-dimensional (2D) mounds which may be simultaneously present on the crystal surface. In typical situations of patterned surfaces, the initial step configuration describes a collection of mounds. During the subsequent surface evolution, these mounds may encroach on one another as they tend to coalesce. In this process, the bases of neighboring mounds touch and possibly merge. Hence, eventually, the bases locally form a monolayer. At this stage of evolution, the steps bounding the bases collide and annihilate. In our geometry of a mound composed of a monotone step train in 1D, at each step annihilation time the most recently completed monolayer takes on the role of the substrate. We choose to use Eq. (9b) to represent a change in the vertical reference frame upon each step annihilation for mathematical convenience; cf. Ref. [14].

Let us also describe the step creation condition. In the setting with a finite mound, used in our step simulations

(Sec. IV C), our approach is to track the mass deposited onto the top terrace without being incorporated into the mound elsewhere in an auxiliary variable,  $m(t)$ . This  $m(t)$  satisfies the initial value problem

$$\frac{dm}{dt} = \frac{F}{2} \left( 1 + \frac{L_{ES} + L_{DF}}{L_{ES} + L_{tot} - x_N} \right) (L_{tot} - x_N - L_{DF}), \quad (10a)$$

$$m(0) = 0. \quad (10b)$$

In this context, we introduce the step creation times,  $s_i$  ( $i = 1, 2, \dots$ ), via the property

$$\lim_{t \rightarrow s_i^-} m(t) = m_{nuc}, \quad (10c)$$

where  $m_{nuc}$  is a phenomenological parameter representing the size of a critical nucleus. We require that

$$x_{N+1}(s_i) = L_{tot} - m_{nuc}, \quad (10d)$$

$$m(s_i) = 0. \quad (10e)$$

The total mass is conserved according to this step creation condition. Note that new steps are created more rapidly when the top terrace is large. The step annihilation and creation conditions imply that the total number of steps, expressed by  $N = N(t)$ , is a discrete, dynamic variable which decreases by 1 when  $t = t_i$  and increases by 1 when  $t = s_i$ .

We should comment on limitations of our model. The main limitation is related to the use of 1D geometries. Equations (9) become more complicated in the realistic setting of truly 2D geometries. In that case, the annihilation process of two colliding steps with opposite signs may in principle not occur simultaneously along the entire steps. This complication cannot be directly incorporated into our model.

In a similar vein, because of our restriction to 1D geometries, our formulation necessarily makes use of an idealized mechanism for nucleation. It is not possible to accurately describe 2D nucleation using a 1D model, even if the nucleation process is taken to be stochastic. For example, the dependence of the nucleation rate for an island in 2D on the length of the boundary cannot be included in our setting.

### C. Rescaling and equations of motion for terrace widths

In this section, we express the step flow model in nondimensional form by use of a suitable length scale for DF. This length enables us to formulate nondimensional equations of motion for the terrace widths. These equations form the focus of most of our analysis in this paper.

We elect to rescale all lengths appearing in the problem by the phenomenological DF length,  $L_{DF}$ ; see Fig. 1. We make this choice anticipating that typically the terrace widths are on the order of  $L_{DF}$ . We also rescale time,  $t$ , by  $Fa$ , where  $F$  is the deposition flux per unit length and  $a$  is the lattice spacing. The effect of the time scaling is that 1 monolayer (ML) of deposition occurs per unit of rescaled time. In regard to the notation, we redefine several frequently used variables as follows:

$$\begin{aligned} x_n &\rightarrow x_n/L_{DF}, & L_n &\rightarrow L_n/L_{DF}, \\ t &\rightarrow Fat, & J_n &\rightarrow J_n/(FL_{DF}). \end{aligned}$$

These replacements persist throughout the paper. Upon making these substitutions, the nondimensional version of Eq. (8a) takes the form

$$\frac{dx_n}{dt} = -(J_n^{\text{int}} + J_n^{\text{dep}}).$$

We now express  $J_n^{\text{int}}$  and  $J_n^{\text{dep}}$  in their nondimensional form, in terms of suitable nondimensional variables. We obtain the following equations for  $J_n^{\text{int}}$ :

$$\begin{aligned} J_n^{\text{int}} &= 2\varepsilon_s \frac{\tilde{c}_{n+1}^{\text{eq}} - \tilde{c}_n^{\text{eq}}}{1 + 2\varepsilon_s(x_n - x_{n-1})} \\ &\quad + 2\varepsilon_s \frac{\tilde{c}_{n-1}^{\text{eq}} - \tilde{c}_n^{\text{eq}}}{1 + 2\varepsilon_s(x_n - x_{n-1})}, \quad n \neq 1, N, \end{aligned} \quad (11a)$$

$$J_1^{\text{int}} = 2\varepsilon_s \frac{\tilde{c}_2^{\text{eq}} - \tilde{c}_1^{\text{eq}}}{1 + 2\varepsilon_s(x_2 - x_1)}, \quad (11b)$$

$$J_N^{\text{int}} = 2\varepsilon_s \frac{\tilde{c}_{N-1}^{\text{eq}} - \tilde{c}_N^{\text{eq}}}{1 + 2\varepsilon_s(x_N - x_{N-1})}, \quad (11c)$$

$$\tilde{c}_n^{\text{eq}} = \tilde{c}^{\text{eq}} \exp\{-\tilde{g}[(x_{n+1} - x_n)^{-3} + (x_n - x_{n-1})^{-3}]\}, \quad n \neq 1, N, \quad (11d)$$

$$\tilde{c}_1^{\text{eq}} = \tilde{c}^{\text{eq}} \exp\{-\tilde{g}(x_2 - x_1)^{-3}\}, \quad (11e)$$

$$\tilde{c}_N^{\text{eq}} = \tilde{c}^{\text{eq}} \exp\{\tilde{g}(x_N - x_{N-1})^{-3}\}. \quad (11f)$$

In the above, we introduce the nondimensional parameters

$$\tilde{c}^{\text{eq}} = \frac{Dc^{\text{eq}}}{FL_{DF}L_{ES}}, \quad (12a)$$

$$\tilde{g} = \frac{2g}{k_B T L_{DF}^2}, \quad (12b)$$

$$\varepsilon_s = \frac{L_{DF}}{2L_{ES}}. \quad (12c)$$

Furthermore, we obtain the following equations for  $J_n^{\text{dep}}$ :

$$J_n^{\text{dep}} = 1 + P_+(L_{n-1})(L_{n-1} - 1) + P_-(L_n)(L_n - 1), \quad n > 1,$$

$$J_1^{\text{dep}} = 1 + L_0 + P_-(L_1)(L_1 - 1).$$

Here, we introduce the *kinetic probabilities*

$$P_-(L_n) = \varepsilon_s \frac{L_n - 1}{1 + 2\varepsilon_s L_n}, \quad n \geq 1, \quad (13)$$

and  $P_+(L_n) = 1 - P_-(L_n)$ , which represent the probabilities for an atom deposited on the  $n$ th terrace to move upward (+) or downward (-). Recall that  $L_0 = x_1$ ,  $L_n = x_{n+1} - x_n$  for  $1 \leq n < N$  and  $L_N = L_{tot} - x_N$ .

### D. Semi-infinite mound

In most of the remainder of this paper, we simplify the analysis without losing sight of the basic physical mechanisms by considering a semi-infinite mound (unless we state otherwise). Hence, the step train extends infinitely to the right (in the positive  $x$  direction) but is terminated at the bottom, on the left (at  $x = 0$ ); see Fig. 1. In this configuration, we seek out the *saturation profile* [13]. This surface profile amounts to an arrangement of step positions that is exactly reproduced after each monolayer of deposition.

In more technical terms, we address the solution of a system of differential equations for the terrace widths subject to the step annihilation condition. In this framework, we seek out a solution to the combined system that has period equal to unity, so that the overall mound profile is reproduced upon each monolayer of deposition. By arbitrarily selecting the saturation profile to be the one that occurs at the exact moment of a step annihilation, we can handle the boundary condition implicitly. Specifically, we require that

$$x_1(1) = 0, \quad (14a)$$

$$x_n(1) = x_{n-1}(0), \quad n \geq 1. \quad (14b)$$

For the time being, we restrict attention to the case with irreversible growth; thus, we set  $J_n^{\text{int}} = 0$  in Eq. (8a). In this situation, we recast Eq. (8a), which governs the (nondimensional) step positions  $x_n$ , into the following equations for the terrace widths,  $L_n$ :

$$\frac{dL_0}{dt} = -L_0 - P_-(L_1)(L_1 - 1) - 1, \quad (15a)$$

$$\frac{dL_1}{dt} = L_0 - [P_+(L_1) - P_-(L_1)](L_1 - 1) - P_-(L_2)(L_2 - 1), \quad (15b)$$

$$\frac{dL_n}{dt} = P_+(L_{n-1})(L_{n-1} - 1) - [P_+(L_n) - P_-(L_n)](L_n - 1) - P_-(L_{n+1})(L_{n+1} - 1), \quad n \geq 2. \quad (15c)$$

We expect that, under the assumption that the slope is selected on a semi-infinite mound, the terrace widths  $L_n$  are asymptotically constant with  $n$ , for large enough  $n$ . Accordingly, we expect that  $P_-(L_n)$  will also be nearly constant for sufficiently large  $n$ . This observation suggests that we might approximate the irreversible step flow model by a simpler model in which the kinetic probabilities  $P_{\pm}$  depend solely on  $\varepsilon_s$  (but not on  $L_n$ ). However, the appropriate dependence of  $P_{\pm}$  on  $\varepsilon_s$  relies on the value of the limit of  $L_n$  as  $n \rightarrow \infty$ , which needs to be determined. In Sec. III, we examine this simplified model, with  $P_{\pm} = \text{constant}$ , under the assumption that  $P_{\pm}$  are prescribed. In Sec. IV, we return to this question on the dependence of the actual  $P_{\pm}$  on  $\varepsilon_s$ .

### III. SIMPLIFIED STEP MODEL: CONSTANT $P_{\pm}$

In this section, we study an implication for slope selection of a simplified, linear version of Eqs. (15). In this version, the probabilities  $P_{\pm}(L)$  are taken to be constants. Our motivation for this simplification is twofold. First, results from this model admit a simple physical interpretation. It has been argued that the behavior of the respective solution retains universal, physically appealing features of the actual epitaxial system [14]. Second, the model of this section is expected to reasonably describe the long-time behavior of the (nonlinear) step flow model in the kinetic regime of a relatively strong ES barrier, when the ES length is larger than the typical terrace width. Third, our analysis of the simplified case has elements that are useful in the treatment of the (more demanding) nonlinear step system.

The simplified system for the terrace widths reads

$$\frac{dL_0}{dt} = -L_0 - P_+ - P_-L_1, \quad (16a)$$

$$\frac{dL_1}{dt} = L_0 - L_1 + P_+ - P_-(L_0 - 2L_1), \quad (16b)$$

$$\frac{dL_n}{dt} = L_{n-1} - L_n - P_-(L_{n-1} - 2L_n + L_{n+1}), \quad n \geq 2. \quad (16c)$$

In the above,  $P_{\pm}$  are given constants with  $P_+ + P_- = 1$ . This model is introduced and studied in Refs. [14–16]. Note that the DF mechanism only appears explicitly in the evolution equations for  $L_0(t)$  and  $L_1(t)$ . Recall that the  $n$ th terrace width,  $L_n$ , is scaled with length  $L_{\text{DF}}$ .

Our goal is to characterize the saturation profile emerging from Eqs. (16). From this characterization, we extract the limiting value of the surface slope. We treat this problem by using the notion of the generating function, by which the linear system of terrace widths is transformed to a complex-valued function,  $G$ . This technique is suitable for the present linear case, but cannot be directly applied to the nonlinear step flow, for which a different approach is warranted. This alternate approach can also be applied to this linear problem. We defer a discussion of this approach to the Appendix.

The technique based on the generating function has been used previously in the context of step flow for slope selection [13,14]. However, these analyses are limited to the case with  $P_- = 0$  [13,14]. In contrast, our approach, despite its perturbative character, ultimately addresses the case for arbitrary constant  $P_-$  with  $0 \leq P_- < 1/2$ .

We exploit the property that for  $P_- = 0$  the system of evolution equations for  $L_n(t)$  exhibits a simple triangular structure. To use this property for  $P_- > 0$ , we treat the terms that are proportional to  $P_-$  as small perturbations. In this framework, the contribution to the solution for the  $n$ th terrace width,  $L_n(t)$ , from a given perturbation order, say,  $k$ , in powers of  $P_-$  involves only  $L_n$  and  $L_{n-1}$  to order  $k$ , and  $L_{n+1}$  to order  $k - 1$ . Thus, the triangular structure of the system manifests to arbitrary order,  $k$ . This attribute allows for a similar treatment (as for  $P_- = 0$ ) of the problem with  $P_- > 0$  in the perturbation scheme. By summation of all orders in  $P_-$ , our results hold for  $0 \leq P_- < 1/2$ .

In more detail, we define the generating function,  $G$ , associated with the sequence of terrace widths,  $L_n(t)$ , by

$$G(\zeta, t) = \sum_{n=0}^{\infty} \zeta^n L_n(t). \quad (17)$$

In this formula,  $\zeta$  is complex and subject to the requirement that the series on the right-hand side converge. By differentiating  $G(\zeta, t)$  with respect to time,  $t$ , and using Eqs. (16), we derive the following evolution equation for  $G(\zeta, t)$ :

$$\frac{\partial G}{\partial t} = (\zeta - 1)G(\zeta, t) + (\zeta - 1)P_+ - P_-(\zeta - 1)^2 \frac{G(\zeta, t) - G(0, t)}{\zeta}, \quad (18a)$$

with initial condition

$$G(\zeta, 0) = R(\zeta) \equiv \sum_{n=0}^{\infty} L_n(0)\zeta^n. \quad (18b)$$

Recall that our objective is to determine the saturation profile. Hence, we seek out an  $R(\zeta)$  such that the solution to Eq. (18a) satisfies  $L_{n+1}(1) = L_n(0)$  for  $n = 0, 1, \dots$  and  $L_0(1) = 0$ . This requirement may be transparently encoded into  $G$  by the statement

$$G(\zeta, 1) = \zeta R(\zeta). \quad (19)$$

To reiterate, the function  $R(\zeta)$  entering the initial condition here is part of the solution of the problem. In fact,  $R(\zeta)$  is the generating function of the saturation profile.

A naive approach to solving Eqs. (18) would be to separate  $G(\zeta, t)$  from its value at  $\zeta = 0$  on the right-hand side and integrate forward in time. This procedure yields a relation for  $G(\zeta, t)$  in terms of the unknown  $R(\zeta)$  and  $G(0, t)$ . However, the separation of  $G(\zeta, t)$  from  $G(0, t)$  creates an artificial singularity in the formula for  $G(\zeta, t)$ . The continuity of  $G(\zeta, t)$  as  $\zeta \rightarrow 0$  dictates that this singularity be removable via imposition of some additional compatibility condition. We choose not to follow this approach here.

We proceed to find  $G(\zeta, t)$  by perturbations, treating the terms involving  $P_-$  in the evolution equations as sufficiently small. To this end, we apply the formal expansion

$$G(\zeta, t) = P_+ \sum_{k=0}^{\infty} P_-^k G_{(k)}(\zeta, t), \quad (20)$$

where the coefficients,  $G_{(k)}$ , are considered as independent of  $P_-$ , and the factor of  $P_+$  is included for later algebraic convenience. The substitution of the above expansion into Eq. (18a) entails the following hierarchy:

$$\frac{\partial G_{(0)}}{\partial t} = (\zeta - 1)G_{(0)}(\zeta, t) + (\zeta - 1), \quad (21a)$$

$$\begin{aligned} \frac{\partial G_{(1)}}{\partial t} &= (\zeta - 1)G_{(1)}(\zeta, t) - (\zeta - 1) \\ &\quad - (\zeta - 1)^2 \frac{G_{(0)}(\zeta, t) - G_{(0)}(0, t)}{\zeta}, \end{aligned} \quad (21b)$$

$$\begin{aligned} \frac{\partial G_{(k)}}{\partial t} &= (\zeta - 1)G_{(k)}(\zeta, t) - (\zeta - 1)^2 \\ &\quad \times \frac{G_{(k-1)}(\zeta, t) - G_{(k-1)}(0, t)}{\zeta}, \quad k \geq 2. \end{aligned} \quad (21c)$$

In Eq. (21b), the term  $-(\zeta - 1)$  arises entirely as a result of the factor of  $P_+$  in Eq. (20).

We now apply initial condition (18b) and periodicity condition (19) through the hierarchy by introducing functions  $R_{(k)}(\zeta)$  as

$$G_{(k)}(\zeta, 0) = R_{(k)}(\zeta)$$

and imposing the requirement

$$G_{(k)}(\zeta, 1) = \zeta R_{(k)}(\zeta). \quad (22)$$

Using Eq. (22), hierarchy (21) can be solved recursively. Integration in time yields

$$G_{(0)}(\zeta, t) = e^{(\zeta-1)t} R_{(0)}(\zeta) + e^{(\zeta-1)t} [1 - e^{(1-\zeta)t}], \quad (23a)$$

$$\begin{aligned} G_{(1)}(\zeta, t) &= e^{(\zeta-1)t} R_{(1)}(\zeta) - e^{(\zeta-1)t} [1 - e^{(1-\zeta)t}] - e^{(\zeta-1)t} \\ &\quad \times (\zeta - 1)^2 \left\{ \int_0^t e^{(1-\zeta)s} \frac{G_{(0)}(\zeta, s) - G_{(0)}(0, s)}{\zeta} ds \right\}, \end{aligned} \quad (23b)$$

$$\begin{aligned} G_{(k)}(\zeta, t) &= e^{(\zeta-1)t} R_{(k)}(\zeta) - e^{(\zeta-1)t} (\zeta - 1)^2 \\ &\quad \times \left\{ \int_0^t e^{(1-\zeta)s} \frac{G_{(k-1)}(\zeta, s) - G_{(k-1)}(0, s)}{\zeta} ds \right\}, \end{aligned} \quad (23c)$$

where  $k \geq 2$  in the last expression. With the dynamics in place, it remains only to compute the functions  $R_{(k)}(\zeta)$  by using Eq. (22). This procedure yields

$$R_{(0)}(\zeta) = \frac{e^{\zeta-1}}{\zeta - e^{\zeta-1}} (1 - e^{1-\zeta}), \quad (24a)$$

$$\begin{aligned} R_{(1)}(\zeta) &= -\frac{e^{\zeta-1}}{\zeta - e^{\zeta-1}} (1 - e^{1-\zeta}) - \frac{(\zeta - 1)^2 e^{\zeta-1}}{\zeta - e^{\zeta-1}} \\ &\quad \times \left\{ \int_0^1 e^{(1-\zeta)s} \frac{G_{(0)}(\zeta, s) - G_{(0)}(0, s)}{\zeta} ds \right\}, \end{aligned} \quad (24b)$$

$$\begin{aligned} R_{(k)}(\zeta) &= -\frac{(\zeta - 1)^2 e^{\zeta-1}}{\zeta - e^{\zeta-1}} \left\{ \int_0^1 ds e^{(1-\zeta)s} \right. \\ &\quad \left. \times \frac{G_{(k-1)}(\zeta, s) - G_{(k-1)}(0, s)}{\zeta} \right\}, \quad k \geq 2. \end{aligned} \quad (24c)$$

Note that Eqs. (23) and (24) cannot be used separately, but must be solved as a system. To illustrate this point, we obtain the following explicit formulas:

$$G_{(0)}(\zeta, t) = e^{(\zeta-1)t} \left[ \frac{e^{\zeta-1}}{\zeta - e^{\zeta-1}} (1 - e^{1-\zeta}) + 1 - e^{(1-\zeta)t} \right], \quad (25a)$$

$$\begin{aligned} R_{(1)}(\zeta) &= \frac{1 - e^{\zeta-1}}{\zeta - e^{\zeta-1}} - \frac{e^{\zeta-1} (\zeta - 1)^2}{\zeta (\zeta - e^{\zeta-1})} \\ &\quad \times \left( \frac{e^{\zeta-1} - 1}{\zeta - e^{\zeta-1}} + 1 + e \frac{e^{-\zeta} - 1}{\zeta} \right), \end{aligned} \quad (25b)$$

$$\begin{aligned} G_{(1)}(\zeta, t) &= e^{(\zeta-1)t} [R_{(1)}(\zeta) - 1 + e^{(1-\zeta)t}] \\ &\quad - \frac{e^{(\zeta-1)t} (\zeta - 1)^2}{\zeta} \left\{ t [R_{(0)}(\zeta) + 1] + e \frac{e^{-\zeta t} - 1}{\zeta} \right\}. \end{aligned} \quad (25c)$$

To continue to obtain expressions for  $R_{(k)}$  and  $G_{(k)}$  for higher  $k$ , use the formula for  $G_{(1)}$  in Eq. (24c) with  $k = 2$  in order to obtain  $R_{(2)}$ , then apply Eq. (23c) to obtain  $G_{(2)}$ , and iterate.

An appealing feature of the surface profile that can be readily extracted from  $R(\zeta)$  by using Eqs. (24) is the asymptotic limit of the slope, i.e., the value  $\lim_{n \rightarrow \infty} (a/L_n)$ . This limit can be computed without the explicit computation of  $R(\zeta)$ . Indeed, notice that

$$\begin{aligned} \lim_{n \rightarrow \infty} L_n(0) &= \lim_{\zeta \rightarrow 1} [(1 - \zeta)R(\zeta)] \\ &= \lim_{\zeta \rightarrow 1} \left[ P_+ (1 - \zeta) \sum_{k=0}^{\infty} P_-^k R_{(k)}(\zeta) \right] \\ &= P_+ \sum_{k=0}^{\infty} P_-^k \lim_{\zeta \rightarrow 1} [(1 - \zeta)R_{(k)}(\zeta)]. \end{aligned}$$

The computation of these limits yields

$$\lim_{\zeta \rightarrow 1} [(1 - \zeta)R_{(k)}(\zeta)] = 2 \lim_{\zeta \rightarrow 1} [(1 - \zeta)R_{(k-1)}(\zeta)], \quad k \geq 1,$$

$$\lim_{\zeta \rightarrow 1} [(1 - \zeta)R_{(0)}(\zeta)] = 2.$$

Hence, we obtain

$$\lim_{\zeta \rightarrow 1} [(1 - \zeta)R_{(k)}(\zeta)] = 2^{k+1}.$$

Accordingly, we compute

$$\lim_{n \rightarrow \infty} L_n = 2P_+ \sum_{k=0}^{\infty} (2P_-)^k = \frac{2P_+}{1 - 2P_-} = \frac{1 + P_+ - P_-}{P_+ - P_-},$$

if  $2P_- < 1$ . Thus, the limiting value of the mound slope,  $m$ , equals

$$m = \lim_{n \rightarrow \infty} \left( \frac{a}{L_n} \right) = a \frac{P_+ - P_-}{1 + P_+ - P_-}, \quad (26)$$

where the lattice spacing,  $a$ , is scaled with  $L_{DF}$ . (Thus, this  $m$  is nondimensional, as it should be.) Equation (26) is a highlight of our analysis.

It should be mentioned that formula (26) has limitations. Evidently,  $P_-$  is not allowed to take the value  $1/2$ , as seen by the geometric series involved in the computation of  $\lim_{n \rightarrow \infty} L_n$  above. In fact, we can argue on physical grounds that Eq. (26) becomes questionable when  $P_-$  is sufficiently close to  $1/2$  and, thus,  $m$  approaches zero. Indeed, in view of Eq. (13), this regime can be reached when the ES barrier is relatively weak, if  $\varepsilon_s L_n \gg 1$  with  $L_n \gg 1$ . In this case,  $m$  is expected to be small, but nonlinearities in step flow are significant; hence, the simplified model of this section may not capture the step dynamics accurately.

Formula (26) has been previously obtained by a flux balance argument [39]. The idea in this argument is to balance out the uphill and downhill fluxes on the  $n$ th terrace with  $n \geq 2$ . The uphill flux results from the condition  $P_+ > P_-$ , while the downhill flux results from the DF mechanism. Equating these fluxes gives  $(P_+ - P_-)(L_\infty - 1) = 1$ , where  $L_\infty$  is the limiting terrace width. The last equation is obeyed by  $L_\infty = am^{-1}$ ; thus, Eq. (26) is recovered. In contrast to the flux balance argument, which appears to be tailored to a (doubly) infinite step train, our analysis here connects the selected slope to the choice of the kinetics for the extremal steps, at the bottom of a semi-infinite mound.

In the present framework of the generating function,  $G$ , the terrace widths,  $L_n(t)$ , can be computed via the expansion

$$L_n(t) = P_+ \sum_{k=0}^{\infty} P_-^k L_{n,(k)}(t),$$

where the coefficients,  $L_{n,(k)}(t)$ , are given by

$$L_{n,(k)}(t) = \frac{1}{n!} \left. \frac{\partial^n G_{(k)}}{\partial \zeta^n} \right|_{\zeta=0} \quad (n = 0, 1, \dots). \quad (27)$$

Evolution equations for  $L_{n,(k)}(t)$  then follow from Eqs. (21). For example, using Eq. (21a) we obtain evolution equations

for  $L_{n,(0)}$ , viz.,

$$\frac{dL_{0,(0)}}{dt} = \left. \frac{\partial G_{(0)}}{\partial t} \right|_{\zeta=0} = -L_{0,(0)}(t) - 1, \quad (28a)$$

$$\frac{dL_{1,(0)}}{dt} = \left. \frac{\partial}{\partial \zeta} \frac{\partial G_{(0)}}{\partial t} \right|_{\zeta=0} = L_{0,(0)}(t) - L_{1,(0)}(t) + 1, \quad (28b)$$

$$\begin{aligned} \frac{dL_{n,(0)}}{dt} &= \left. \frac{1}{n!} \frac{\partial^n}{\partial \zeta^n} \frac{\partial G_{(0)}}{\partial t} \right|_{\zeta=0} \quad (n \geq 2) \\ &= \left. \frac{n}{n!} \frac{\partial^{n-1}}{\partial \zeta^{n-1}} \frac{\partial G_{(0)}}{\partial t} \right|_{\zeta=0} - \left. \frac{1}{n!} \frac{\partial^n}{\partial \zeta^n} \frac{\partial G_{(0)}}{\partial t} \right|_{\zeta=0} \\ &= L_{n-1,(0)}(t) - L_{n,(0)}(t). \end{aligned} \quad (28c)$$

Alternatively, these equations may be derived directly from dominant balance arguments, without the use of the generating function. We carry out this approach for the present setting in the Appendix. We also apply this approach to the nonlinear step flow model in Sec. IV A.

Similarly, we can invoke approximations for  $R(\zeta)$  to derive approximate formulas for the saturation profile, by using identity (27) at  $t = 0$ . With  $k = 0$ , Eq. (24a) yields the general expression

$$L_{n,(0)} = \sum_{m=0}^n (-1)^m \frac{(n+1-m)^m e^{n+1-m} - (n-m)^m e^{n-m}}{m!}.$$

This expression is obtained via expanding  $(\zeta - e^{\zeta-1})^{-1}$  in powers of  $\zeta$  for  $|\zeta| < 1$ . A few particular values of  $L_{n,(0)}$  (for  $n = 0, 1, 2$ ) are given here:

$$L_{0,(0)} = e - 1 \approx 1.718,$$

$$L_{1,(0)} = e^2 - 2e \approx 1.952,$$

$$L_{2,(0)} = e^3 - 3e^2 + \frac{3}{2}e \approx 1.9958.$$

In principle, one can apply a similar procedure for Eq. (25b) in order to obtain expressions for the coefficients  $L_{n,(1)}$ , but the procedure is more cumbersome. For example, the values of  $L_{n,(1)}$  involving just the first two terraces ( $n = 0, 1$ ) are found to be

$$L_{0,(1)} = 1 - \frac{5e}{2} + e^2 \approx 1.593,$$

$$L_{1,(1)} = \frac{e}{6}(38 - 45e + 12e^2) \approx 1.969.$$

#### IV. NONLINEAR STEP FLOW MODEL IN IRREVERSIBLE GROWTH

In this section, we focus on the nonlinear step flow model under irreversible growth. We repeat that in this setting the equilibrium adatom density at every step is nearly zero, viz.,  $c_n^{\text{eq}} \simeq 0$  at the  $n$ th step in kinetic relation (2). We integrate Eqs. (15) for the evolving terrace widths with definitions (12c) and (13). Our goal is to approximately characterize the saturation profile. In our approach, we treat the parameter  $\varepsilon_s$  as small. First, we formulate an explicit iterative scheme. Second, we provide and discuss numerical computations using this scheme.

### A. Iterative method: Formulation

For later algebraic convenience, we define the quantity

$$Q(L) = \varepsilon_s^{-1} P_-(L) = \frac{L-1}{1+2\varepsilon_s L}. \quad (29)$$

By use of this  $Q$ , Eqs. (15) read

$$\frac{dL_0}{dt} = -L_0 - 1 - \varepsilon_s Q(L_1)(L_1 - 1), \quad (30a)$$

$$\frac{dL_1}{dt} = L_0 - L_1 + 1 + 2\varepsilon_s Q(L_1)(L_1 - 1) - \varepsilon_s Q(L_2)(L_2 - 1), \quad (30b)$$

$$\frac{dL_n}{dt} = L_{n-1} - L_n - \varepsilon_s Q(L_{n-1})(L_{n-1} - 1) + 2\varepsilon_s Q(L_n) \times (L_n - 1) - \varepsilon_s Q(L_{n+1})(L_{n+1} - 1), \quad n \geq 2. \quad (30c)$$

Next, we consider the expansion

$$L_n(t) = \sum_{k=0}^{\infty} \varepsilon_s^k L_n^{(k)}(t) \quad (n \geq 0), \quad (31)$$

where the coefficients  $L_n^{(k)}(t)$  are treated as independent of  $\varepsilon_s$ . The substitution of this expansion for  $L_n(t)$  into Eqs. (30) leads to hierarchical equations of motion for the associated coefficients,  $L_n^{(k)}$ . To carry out this program, we need to group the ensuing terms on the right-hand sides of Eqs. (30) according to their order in  $\varepsilon_s$ . Caution should be exercised in handling the nonlinear terms  $Q(L_n)(L_n - 1)$  since these terms must be expanded in powers of  $\varepsilon_s$  as well.

We now describe evolution equations for  $L_n^{(k)}$  up to second order in  $\varepsilon_s$ , i.e., for  $k = 0, 1, 2$ , while we keep  $n$  fixed. To carry out this task, we need a suitable approximation for  $Q(L_n)(L_n - 1)$ . Recalling (29), we have

$$Q(L_n)(L_n - 1) = \frac{(L_n - 1)^2}{1 + 2\varepsilon_s L_n} = (L_n^{(0)} - 1)^2 - 2\varepsilon_s (L_n^{(0)} - 1) \times [(L_n^{(0)})^2 - L_n^{(0)} - L_n^{(1)}] + \mathcal{O}(\varepsilon_s^2).$$

The symbol  $\mathcal{O}(\varepsilon_s^2)$  implies that the remainder of the respective expansion is of second order in the small parameter,  $\varepsilon_s$ .

We substitute the above approximation for the quantity  $Q(L_n)(L_n - 1)$  into Eqs. (30) and invoke the principle of dominant balance. We obtain the following equations for  $L_n^{(k)}$  ( $k = 0, 1, 2$ ):

$$\frac{dL_0^{(0)}}{dt} = -L_0^{(0)} - 1, \quad (32a)$$

$$\frac{dL_1^{(0)}}{dt} = L_0^{(0)} - L_1^{(0)} + 1, \quad (32b)$$

$$\frac{dL_n^{(0)}}{dt} = L_{n-1}^{(0)} - L_n^{(0)}, \quad n \geq 2, \quad (32c)$$

$$\frac{dL_0^{(1)}}{dt} = -L_0^{(1)} - (L_1^{(0)} - 1)^2, \quad (32d)$$

$$\frac{dL_1^{(1)}}{dt} = L_0^{(1)} - L_1^{(1)} + 2(L_1^{(0)} - 1)^2 - (L_2^{(0)} - 1)^2, \quad (32e)$$

$$\frac{dL_n^{(1)}}{dt} = L_{n-1}^{(1)} - L_n^{(1)} - (L_{n-1}^{(0)} - 1)^2 + 2(L_n^{(0)} - 1)^2 - (L_{n+1}^{(0)} - 1)^2, \quad n \geq 2, \quad (32f)$$

$$\frac{dL_0^{(2)}}{dt} = -L_0^{(2)} + 2(L_1^{(0)} - 1)[(L_1^{(0)})^2 - L_1^{(0)} - L_1^{(1)}], \quad (32g)$$

$$\frac{dL_1^{(2)}}{dt} = L_0^{(2)} - (L_1^{(2)} - 1) + 2(L_2^{(0)} - 1) \times [(L_2^{(0)})^2 - L_2^{(0)} - L_2^{(1)}] - 4(L_1^{(0)} - 1)[(L_1^{(0)})^2 - L_1^{(0)} - L_1^{(1)}], \quad (32h)$$

$$\frac{dL_n^{(2)}}{dt} = L_{n-1}^{(2)} - L_n^{(2)} + 2(L_{n-1}^{(0)} - 1) \times [(L_{n-1}^{(0)})^2 - L_{n-1}^{(0)} - L_{n-1}^{(1)}] - 4(L_n^{(0)} - 1)[(L_n^{(0)})^2 - L_n^{(0)} - L_n^{(1)}] + 2(L_{n+1}^{(0)} - 1) \times [(L_{n+1}^{(0)})^2 - L_{n+1}^{(0)} - L_{n+1}^{(1)}], \quad n \geq 2. \quad (32i)$$

We also impose the following terminal conditions:

$$L_0^{(k)}(1) = 0, \quad (33a)$$

$$L_n^{(k)}(1) = L_{n-1}^{(k)}(0), \quad n \geq 1, \quad k = 0, 1, 2, \quad (33b)$$

which ensure that, to the desired order of perturbation theory,  $L_n(0)$  is the saturation profile as defined previously.

Before moving on to the solution of the aforementioned problem, we inspect the structure of Eqs. (32). It is clear that the zeroth-order problem (with  $k = 0$ ) of the present formulation, expressed by Eqs. (32a)–(32c), is the same as the corresponding problem for the simplified, linear step flow model of constant probabilities, with  $P_+ = 1$  and  $P_- = 0$  (see Sec. III). In particular, there is no downward transport except for DF. These equations can be integrated exactly by exploiting their triangular structure. For this development, see the Appendix.

Equations (32d)–(32i) introduce the effects of downward transport other than DF through additional forcing terms. These terms involve coefficients from the previous perturbation orders, and thus take into account the fact that the amount of downward transport depends on the terrace widths.

We now discuss in some detail the solution to Eqs. (32d)–(32i). We solve these evolution equations recursively. In each case, we use  $e^t$  as an integrating factor, and integrate the equation from the final time,  $t = 1$ , to the observation time,  $t$ . For  $k = 1$ , this procedure yields the following relations:

$$L_0^{(1)}(t) = -e^{-t} \int_1^t e^s [L_1^{(0)}(s) - 1]^2 ds, \quad (34a)$$

$$L_1^{(1)}(t) = e^{-t} \left\{ e L_0^{(1)}(0) + \int_1^t ds e^s [L_0^{(1)}(s) + 2[L_1^{(0)}(s) - 1]^2 - (L_2^{(0)} - 1)^2] \right\}, \quad (34b)$$

$$L_n^{(1)}(t) = e^{-t} \left\{ e L_{n-1}^{(1)}(0) + \int_1^t ds e^s [L_{n-1}^{(1)} - [L_{n-1}^{(0)}(s) - 1]^2 + 2[L_n^{(0)}(s) - 1]^2 - [L_{n+1}^{(0)}(s) - 1]^2] \right\}, \quad n \geq 2. \quad (34c)$$

The analogous formulas to the next perturbation order,  $k = 2$ , can be derived similarly but are omitted here for the sake of brevity.

The analytical formalism of this subsection, although increasingly cumbersome with the perturbation order,  $k$ , is amenable to numerical computations. (This task is addressed in Sec. IV B.)

### B. Iterations: Numerical results and effective model

Next, we use the iterative method formulated in Sec. IV A in order to study the behavior of terrace widths in slope selected profiles. Overall we obtain two appealing results. First, the contribution to the terrace widths from the second-order terms in perturbation theory are quite small, even when  $\varepsilon_s$  becomes relatively large (of the order of unity). Second, the first-order results compare favorably to the results of direct numerical simulations of the step flow model.

In principle, the iterative scheme involves integrals that may be evaluated analytically, but this procedure becomes increasingly cumbersome after just a few iterations. Thus, we evaluate these integrals numerically. We also carry out a similar computation for the simplified model of constant probabilities (Sec. III). Notably, because this simplified model is linear, it is straightforward to carry out the computation to arbitrary order in perturbations. We take advantage of this property to obtain accurate results for this model even if  $P_-$  takes values close to  $1/2$ .

The results of our iterative procedure are summarized in Fig. 2, which shows the outcomes of the perturbative expansions for the first few terrace widths as functions of  $\varepsilon_s$  and  $P_-$ . Figure 2 clearly indicates that the terrace widths, at least when computed to second order in perturbation theory, are almost linear functions of  $\varepsilon_s$ ; i.e., the coefficients  $L_n^{(2)}$  are negligibly small. In Table I, we show the coefficients,  $L_n^{(k)}$ , that generate the expansion for the step flow model, as well as a few of the coefficients for the simplified model of constant probabilities. Evidently,  $L_n^{(2)}$  are found to be relatively small for  $n \geq 1$ .

In view of these results, we identify

$$L_n \simeq L_\infty = 2 + 2\varepsilon_s, \quad n \gg 1, \quad (35)$$

TABLE I. Terrace width expansion coefficients,  $L_n^{(k)}$ , in saturation profile, for irreversible and simplified step flow models (as indicated inside parentheses of first row); see Eq. (31). Note that  $L_n^{(0)}$  is the same in each model. The expansion order,  $n$ , takes values with  $n \leq 9$  while the perturbation order is  $k = 0, 1, 2$ .

$n$	$L_n^{(0)}$	$L_n^{(1)}$ (simp.)	$L_n^{(1)}$ (step)	$L_n^{(2)}$ (simp.)	$L_n^{(2)}$ (step)
0	1.71828183	1.59335153	1.49638475	3.24895018	0.16583988
1	1.95249244	1.96893802	1.98136495	3.93330269	-0.00679066
2	1.99579137	2.00125417	2.00658950	3.99630281	-0.02393955
3	2.00003885	2.00002908	2.00006258	3.99980897	-0.00130086
4	2.00005758	1.99987984	1.99970687	4.00009654	0.00130010
5	2.00000507	1.99998206	1.99995886	4.00002838	0.00025839
6	1.99999964	2.00000106	2.00000239	3.99999957	-0.00000911
7	1.99999989	2.00000056	2.00000123	3.99999882	-0.00000911
8	1.99999999	2.00000004	2.00000009	3.99999986	-0.00000089
9	2.00000000	1.99999999	1.99999998	4.00000002	0.00000013

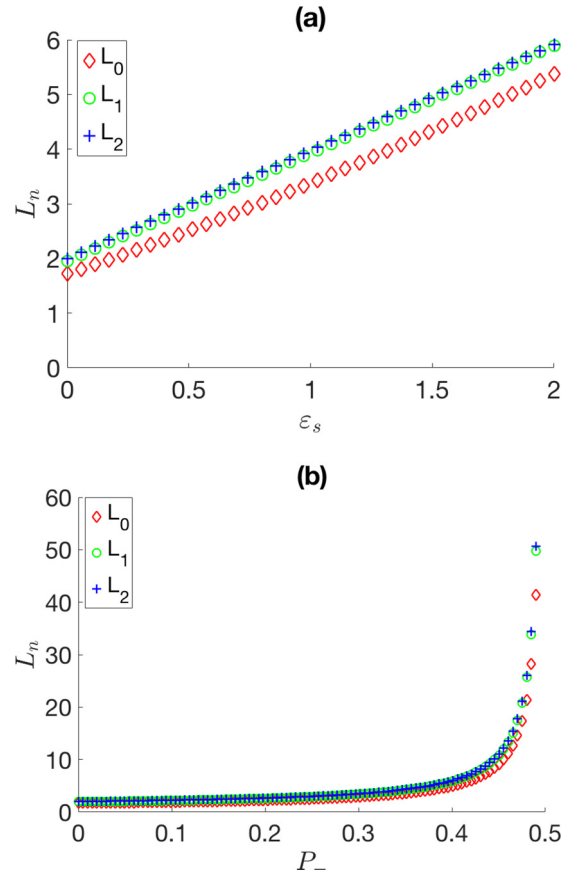


FIG. 2. Plots of terrace widths,  $L_n$ , in the saturation profile for (a) the irreversible step flow model of Eqs. (30), in which  $L_n$  is viewed as a function of  $\varepsilon_s$  (top panel), and (b) the simplified step flow model of Eqs. (16) where  $L_n$  is viewed as a function of probability  $P_-$  (bottom panel).

which we consider as a reasonable approximation for the terrace widths, in the large- $n$  asymptotic regime of the irreversible step flow model.

Next, we provide two intuitive explanations for the relatively small values of the coefficients  $L_n^{(2)}$  of the perturbation expansion in the step flow model, as well as for the reason

why the ensuing first-order approximation may be expected to exactly take the form of Eq. (35).

First, we consider a flux balance argument, analogous to the argument used to obtain Eq. (26) for the simplified model of Sec. III. In this case, the balance equation reads

$$1 + \varepsilon_s \frac{(L-1)^2}{1 + 2\varepsilon_s L} = \left(1 - \varepsilon_s \frac{L-1}{1 + 2\varepsilon_s L}\right)(L-1), \quad (36)$$

which exactly yields  $L = 2 + 2\varepsilon_s$ . A similar derivation of this result has been given previously in [13]. We remind the reader that the flux balance argument here is local, as it involves the terrace width away from extremal steps. In other words, this argument leaves out the different behavior of steps at the bottom of the mound.

Second, we make a systematic attempt to establish a closer connection between the step flow model of this section and its simplified version of constant probabilities (Sec. III). Consider the simplified model with the value of  $P_-$  determined from Eq. (13), where the value of  $L_n$  comes from applying the zeroth-order approximation and taking the limit  $n \rightarrow \infty$ . We already established that the result of this procedure is  $L_\infty = 2$ . This result in turn suggests that, at least for small  $\varepsilon_s$ , we may approximate the slope selected profile arising in the step flow model by considering *instead* the simplified model with

$$P_- = \frac{\varepsilon_s}{1 + 4\varepsilon_s}.$$

Equation (26) with this value of  $P_-$  entails the limit

$$\lim_{n \rightarrow \infty} L_n = \frac{2 + 6\varepsilon_s}{1 + 2\varepsilon_s}. \quad (37)$$

This approximation agrees with Eq. (35) to first order in  $\varepsilon_s$ . In this regard, we may consider the simplified model with  $P_-$  chosen to be equal to  $\varepsilon_s/(1 + 4\varepsilon_s)$  to be an *effective model* for the irreversible step flow model in the small- $\varepsilon_s$  regime. This characterization is one of the key results of our analysis.

### C. Step simulations

In this subsection, we compare the results of direct integration of the ordinary differential equations (ODEs) for terrace widths in the nonlinear step flow model to our perturbation analysis of the saturation profile. To this end, we assume that the mound is finite. This assumption implies that we must include a mechanism for the creation of steps on top of the mound in order to account for slope selection. Bearing in mind that no 1D nucleation model is physically compelling, we resort to the nucleation condition described in Eqs. (10) for irreversible growth.

In Fig. 3, we show the average terrace width, viz.,

$$\frac{1}{N(t) + 1} \sum_{n=0}^{N(t)} L_n(t),$$

in snapshots of the irreversible step flow model (at several time instants) for various values of parameter  $\varepsilon_s$ , which expresses the relative strength of the DF effect and ES barrier. We compare these results to the analytical prediction  $a/m = 2 + 2\varepsilon_s$ . In regard to the nucleation condition used in the simulations, we set  $m_{\text{nuc}} = 1 + \varepsilon_s$  and apply the initial conditions  $m(0) = 0$  and  $L_n(0) = 11$  for all  $n$ . In addition,

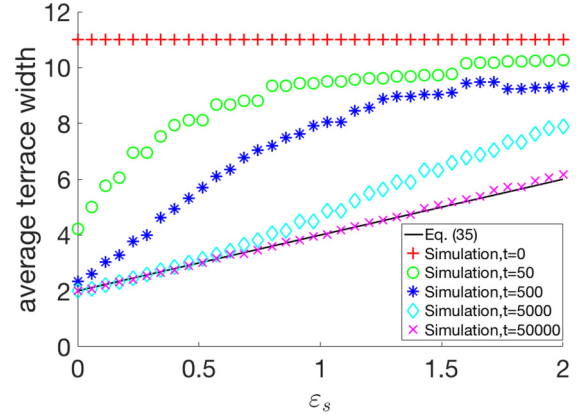


FIG. 3. Comparison of the analytical prediction  $\lim_{n \rightarrow \infty} L_n = 2 + 2\varepsilon_s$  of Eq. (35) in saturation profile to results of numerical simulations for irreversible step flow under nucleation conditions (10) which involve the mass  $m(t)$  and nucleation parameter  $m_{\text{nuc}}$ . The prescribed initial conditions are  $m(0) = 0$  and  $L_n(0) = 11$  for  $n = 0, 1, \dots, N$ , and  $m_{\text{nuc}} = 1 + \varepsilon_s$ . The prescribed number,  $N$ , of initial terraces is taken to increase linearly with  $\varepsilon_s$ .

we linearly increase the number,  $N$ , of initial terraces as  $\varepsilon_s$  increases. By scaling  $m_{\text{nuc}}$  with  $\varepsilon_s$ , we enable slope selection. Similarly, by scaling the overall system size with  $\varepsilon_s$ , we reduce the effect of the extremal steps on the average terrace width in the large- $\varepsilon_s$  step simulations.

The results of our step flow simulations for sufficiently long times,  $t$ , are found to be in reasonably good agreement with the analytical prediction of Eq. (35) for the terrace widths (see Fig. 3). The discrepancy between the analytical prediction and the short-time snapshots can be considered to be due to transient behavior. For large enough  $\varepsilon_s$ , even the long-time snapshot demonstrates some deviation. This can be attributed to the breakdown of slope selection. In this regime, the widths,  $L_n$ , of terraces far away from the extremal steps are significantly different from the widths of terraces near the domain boundaries.

## V. REVERSIBLE GROWTH: STEP-STEP INTERACTIONS

In this section, we examine a more general version of the step flow model, centered around Eqs. (8), which includes the effect of repulsive step-step interactions (see Sec. II A). We consider reversible growth; i.e., the  $n$ th step equilibrium density,  $c_n^{\text{eq}}$ , of adatoms is now a function of terrace widths. Thus, in principle, we have a nonzero flux  $J_n^{\text{int}}$ . Here, we briefly outline the incorporation of step-step interactions into the equations of motion for the terrace widths and carry out step simulations for finite mounds, using the step creation condition introduced in Eqs. (10).

The contribution of step-step interactions to the step velocity law comes from the incorporation of Eqs. (4) into step flow. In particular, the step chemical potential,  $\mu_n$ , is the variational derivative of elastic-dipole energy (4c), in a discrete setting. When the height and width of the (finite) mound are held fixed, this energy is minimized if all terraces except the top and bottom terraces have the same width, while the top and bottom terraces are arbitrarily small. This statement relies on

the assumption that the top and bottom steps, which have positions  $x_1$  and  $x_N$ , only interact (repulsively) with steps that are their nearest neighbors in the same step train; these neighboring steps are located at  $x = x_2, x_{N-1}$ , respectively. This property follows from Eqs. (11e) and (11f). We choose not to implement more complicated scenarios, e.g., the possibility that  $x_1$  interacts with a step of the opposite sign in a neighboring mound.

Let us now intuitively discuss what is the possible effect of step-step interactions on the dynamics of terrace widths in the presence of DF, and the resulting slope selection. Overall, we expect that these interactions tend to render more uniform the widths of terraces that are sufficiently far from the domain boundaries, cause an increase to the speed of the bottom step, and reduce the speed of the top step. The effect of the interactions on the terraces away from the boundaries is expected to be minor, because the kinetic processes under consideration (with DF included) already contribute significantly to the same effect; see Sec. IV. On the other hand, the effect of step-step interactions on terraces near the boundaries may be significant, and indeed may cause the reduction of the average mound slope, by accelerating the rate of step annihilation and slowing the rate of step creation.

Our numerical findings by step simulations for finite mounds are displayed in Fig. 4. In these plots, we show snapshots of the terrace width,  $L_n(t)$ , versus  $n$  at times  $t = 500$  and  $t = 5 \times 10^4$ . Recall the definitions of nondimensional parameters  $\tilde{c}^{\text{eq}}$ ,  $\tilde{g}$ , and  $\varepsilon_s$  introduced in Eqs. (12), and the parameter  $m_{\text{nuc}}$  entering the step creation conditions of Eqs. (10). In the step simulations we set  $\tilde{c}^{\text{eq}} = 10$ ,  $\varepsilon_s = 1/2$ , and  $m_{\text{nuc}} = 1.5$ , while we vary  $\tilde{g}$  by using the values  $\tilde{g} = 0, 1, 5, 10$ . Furthermore, we apply the initial conditions that the step train, or mound, has linear size equal to  $L_{\text{tot}} = 300$  and consists of  $N = 50$  terraces with equal width, where all lengths are scaled by the DF length,  $L_{\text{DF}}$ . Note that the case with  $\tilde{g} = 0$  (vanishing step-step interactions) amounts to the irreversible case (Sec. IV). The other simulations, for  $\tilde{g} \neq 0$ , show the effect of increasing, nonzero strength of step-step repulsion (Fig. 4). To avoid distorting the vertical scale of our plots, we choose to exclude the top and bottom terrace widths from the results of Fig. 4.

In particular, in Fig. 4(a), we present the terrace width,  $L_n(t)$ , as a function of  $n$  at a relatively short time,  $t$ , for several values of  $\tilde{g}$ . Evidently, the step interaction affects the dynamics of slope selection in a way that is more complicated than the simple intuitive argument given above would suggest. In particular, we notice that the changes in  $L_n$ , relative to the case with  $\tilde{g} = 0$ , do not have the same sign along the step train, as a function of  $n$ . We also notice that the changes in  $\tilde{g}$  have a small but detectable effect on  $L_n$  far away from the domain boundaries. Nonetheless we see that the most prominent effects are near the extremal steps, as expected.

The long-time behavior of  $L_n$  observed in Fig. 4(b) indicates the intuitively expected effects of step-step interactions. In fact, we notice that the step profile in the reversible case resembles the one of the irreversible case far away from the boundaries. In particular, the terrace widths away from the mound top and bottom have values close to  $L_\infty = 3$  which is predicted by Eq. (35) with  $\varepsilon_s = 1/2$ . Near the boundaries, however, the step interactions drive the

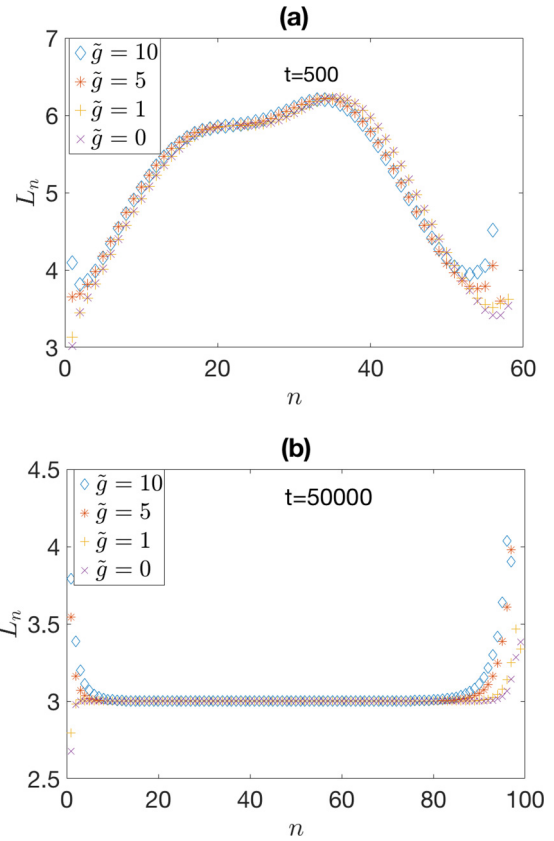


FIG. 4. Terrace width,  $L_n(t)$ , versus  $n$  for fixed times,  $t$ , in the context of the reversible step flow model of Eqs. (8), in the presence of repulsive step-step interactions. Plots are shown at times (a)  $t = 500$  and (b)  $t = 50000$ . The (scaled) interaction strength,  $\tilde{g}$ , varies;  $\tilde{g} = 0, 1, 5, 10$ . In all simulations, we set  $\tilde{c}^{\text{eq}} = 10$ ,  $\varepsilon_s = 1/2$ , and  $m_{\text{nuc}} = 1.5$ ; cf. Eqs. (10) and (12). We use the initial conditions  $x_n(0) = 6n$  for  $n = 1, 2, \dots, 49$ , and  $m(0) = 0$  for mass variable  $m(t)$ ; and the system linear size  $L_{\text{tot}} = 300$ .

extremal terraces to be significantly wider than in the irreversible case. This effect increases essentially monotonically with  $\tilde{g}$ . Moreover, the step interactions affect the overall mound slope only slightly, for the values of  $\tilde{g}$  used in our step simulations ( $\tilde{g} = 0, 1, 5, 10$ ). In fact, the long-time snapshots of  $L_n(t)$  for  $\tilde{g} = 0, 1$  contain 100 steps while the corresponding snapshots for  $\tilde{g} = 5, 10$  contain 98 steps. However, it should be pointed out that this situation may change significantly for much larger values of  $\tilde{g}$ . By inspection of the step velocity law, let us recall that the step dynamics result from the competition of mass fluxes  $J_n^{\text{int}}$  and  $J_n^{\text{dep}}$  (see Sec. II C). For sufficiently strong step interactions,  $J_n^{\text{int}}$  may dominate, thus suppressing the effect of DF which is present in  $J_n^{\text{dep}}$ . This extreme regime of the step interaction parameter,  $\tilde{g}$ , lies beyond our present scope.

## VI. DISCUSSION

In this section, we discuss a few open problems related to the dynamics of step trains in the presence of DF. First, we outline ingredients of the step flow model with DF in radial geometries, when the steps form concentric circles [32].

Second, we describe aspects of continuum limits for evolving stepped surfaces by including DF, as a possible extension to previous similar works, e.g., [7]. Third, we list a few open problems inspired by our work.

### A. Radial geometry

Consider an axisymmetric mound that consists of a stack of concentric circular islands at positions  $r = r_n(t)$ , where  $r$  is the distance from the axis of the mound. We can now formulate a step flow model in a fashion analogous to the setting with straight steps (Sec. II). Suppose that step-step interactions are neglected in the definition of the step chemical potential,  $\mu_n$ . Accordingly, the equations of motion for the nonextremal steps read

$$\begin{aligned} \frac{dr_n}{dt} = & Fa[L_{\text{DF}} + P_{+,n}(r_n - r_{n-1} - L_{\text{DF}})] \\ & + Fa[P_{-,n+1}(r_{n+1} - r_n - L_{\text{DF}})] \\ & + D \left( \frac{c_{n+1}^{\text{eq}} - c_n^{\text{eq}}}{d_{n+1}} + \frac{c_{n-1}^{\text{eq}} - c_n^{\text{eq}}}{d_n} \right), \end{aligned}$$

where  $P_{+,n} + P_{-,n} = 1$ , and

$$\begin{aligned} P_{-,n} = & \frac{1}{2d_n} \left\{ \frac{1}{2} [(r_n - L_{\text{DF}})^2 - (r_{n-1})^2] \left( 1 + \frac{2L_{\text{ES}}}{r_n} \right) \right. \\ & \left. + (r_n - L_{\text{DF}})^2 \ln \left( \frac{r_n}{r_n - L_{\text{DF}}} \right) - (r_{n-1})^2 \ln \left( \frac{r_n}{r_{n-1}} \right) \right\}, \\ d_n = & [r_{n-1}(r_n - r_{n-1} - L_{\text{DF}})] \left[ \frac{L_{\text{ES}}}{r_n} + \ln \left( \frac{r_n}{r_{n-1}} \right) \right], \\ c_n^{\text{eq}} = & c^{\text{eq}} \exp \left( \frac{\tilde{\beta}}{k_B T} r_n^{-1} \right). \end{aligned}$$

Additional terms can be included in the equations of motion for the step radii,  $r_n(t)$ , in order to account for the step-step interactions [3]. The ensuing ODE system for  $r_n(t)$  is amenable to a perturbation method akin to the one in Sec. IV. This task is not addressed here.

A similar system of equations for the step radii appears in Ref. [40]. However, in the 2D geometry, the description of step annihilation is complicated. It is worthwhile to note that in the 1D geometry one can visualize the situation in which two parallel straight steps of opposite sign simply collide and geometrically annihilate one another. In contrast, in 2D settings the process of step annihilation may not be described in this fashion; in particular, the radial character of the geometry may not possibly be preserved after two neighboring mounds collide. In Ref. [40], the authors circumvent this difficulty via a mechanism by which bottom islands annihilate when they reach a critical radius. The demanding problem of island or step annihilation in 2D geometries is not further discussed in the present paper.

### B. Continuum limits of step train with DF

The step flow models discussed hitherto are amenable to corresponding (heuristic) continuum limits in the surface region away from the extremal steps. For example, consider the 1D geometry of Fig. 1, with a monotone step train. The

key idea is to identify each terrace width,  $L_n(t)$ , with  $\rho(x, t)^{-1}$ , where  $\rho$  is a local step density as a function of the spatial coordinate,  $x$ , and time,  $t$ ; or, equivalently, with  $a(\partial h/\partial x)^{-1}$ , where  $a$  is the lattice spacing and  $h(x, t)$  is the local height [5–7]. Let us focus on the irreversible step flow (Sec. IV). Upon appropriately scaling out the deposition rate,  $F$ , and the DF length,  $L_{\text{DF}}$ , and carrying out local Taylor expansions, the resulting continuum evolution law, or partial differential equation (PDE), for the step density is

$$\frac{\partial \rho}{\partial t} = \frac{1}{2} \frac{\partial^2}{\partial x^2} \left[ \frac{1 + 2\varepsilon_s}{1 + 2\varepsilon_s \rho^{-1}} (\rho^{-1} - 1) \right]. \quad (38a)$$

Alternatively, one can obtain a second-order PDE for  $h(x, t)$ . Notably, in the presence of repulsive step-step interactions between straight steps, one can obtain a fourth-order PDE for  $\rho(x, t)$  or  $h(x, t)$ . In regard to the requisite boundary conditions, let us consider a semi-infinite step train. A heuristic argument may specify a boundary condition at the bottom of the mound. Such a condition would state that the rate of loss of steps at the bottom of the mound is given by  $-\rho v$  where  $v$  is the continuum-scale (negative) step velocity at the base of the mound. This formulation suggests a boundary condition of the form

$$\begin{aligned} & \frac{\partial}{\partial x} \left[ \frac{1 + 2\varepsilon_s}{1 + 2\varepsilon_s \rho^{-1}} (\rho^{-1} - 1) \right] \Big|_{x=0} \\ & = \rho \left( 1 + \frac{1 + 2\varepsilon_s}{1 + 2\varepsilon_s \rho^{-1}} \right) (\rho^{-1} - 1) \Big|_{x=0}. \end{aligned} \quad (38b)$$

Equations (38) form a plausibly well-posed continuum theory for slope selection in the presence of DF. We believe that the use of a boundary condition along the lines of Eq. (38b) renders such a theory distinct from otherwise similar theories using periodic boundary conditions [30,31]. However, we should point out that Eq. (38b) in particular is actually not consistent with the step dynamics near the base of the mound, which display a truly discrete character. For an analogous situation in faceted crystals, in which individual steps may affect the surface profile macroscopically, see, e.g., [41,42]. Step flow simulations suggest that the discrete step density is usually significantly higher at the base of the mound than farther away. As a result, boundary condition (38b) may grossly overestimate the rate of step loss. This pathology can be recognized more easily in the extreme case with  $L_{\text{DF}} = 0$  and  $P_- = 0$ , when no downward transport occurs. In this case, there is a ‘‘Zeno effect,’’ which is known to prevent the bottom step from ever annihilating [14]. This effect is an artifact of the step flow model, but even from the atomistic point of view, the annihilation of the bottom step should be very slow in this case. By contrast, the annihilation of the bottom step occurs at a lower-bounded rate according to PDE (38a) with boundary condition (38b).

In principle, if the step annihilation times,  $t_j$ , were known for a given initial step configuration, then one could identify an appropriate continuous variable, say,  $\ell(t)$ , such that  $\ell(t_j) = j$ . This  $\ell(t)$  would count the number of steps that have annihilated. The modification of boundary condition (38b) so that the overall loss of steps after time  $t$  is  $\ell(t)$  would presumably remove most of the discrepancy between the heuristic continuum limit and the underlying, discrete step

model. The program of constructing the continuum-scale  $\ell(t)$  from the sequence  $\{t_j\}$  is left for future work.

### C. Other open problems

We close this section by outlining a couple of other problems related to slope selection that are inspired by but left open in our analysis. Our purpose is to motivate future investigations in the context of slope selection via step flow.

First, consider the dynamical system described by the high-dimensional vector  $\vec{L}(t) = (L_0(t), L_1(t), \dots, L_N(t))$ , which consists of all terrace widths of a finite mound. Admittedly, we still lack an analytical understanding of slope selection from the viewpoint of the subsampled dynamical system  $\vec{L}(t_j)$ , where  $t_j$  is the time of the  $j$ th step creation or annihilation event. Our analysis does not help in analyzing the dynamics of this system; we only construct its fixed point. The difficulty in studying the dynamics in question is that the overall dynamical system  $\vec{L}(t)$  is not truly continuous, because of the step creation and annihilation processes. Thus, the ostensibly straightforward goal of showing that there is an attracting orbit of period 1 is in fact quite challenging. If  $\vec{L}(t_j)$  were given explicitly, then this question would be converted to the perhaps easier task of showing that the fixed point of this system is attracting [43].

A means of dealing with the above difficulty and studying the dynamics of the continuous system would be to give some asymptotic characterization of the time of the  $j$ th nucleation event and the  $j$ th annihilation event for large  $j$ . Then, one could possibly modify the continuum limit of Sec. VI B through a change of the time variable in order to more accurately resolve the total number of steps in the system. This task is left unresolved in the present paper.

Another problem of interest concerns the creation of steps by nucleation of islands. Although our numerical simulations incorporate nucleation on top of mounds, our analysis excludes it, as a result of the use of a semi-infinite mound; see Sec. II. However, in certain systems such as Ag (100) at 300 K, the kinetics of step creation may be the dominant contribution to slope selection [14]. In principle, it would be interesting to extend our analytical framework to take into account step creation. In this direction, difficulties arise because one must treat either step creation or annihilation explicitly. By contrast, the analysis in Sec. III and Sec. IV treats annihilation implicitly for purposes of finding the saturation profile. Moreover, nucleation of islands on terraces other than the top terrace can occur, in which case the step train is no longer monotone. This possibility is not considered in this paper, and should be expected to be relevant in the regime of small slopes (respectively large terrace widths) [13,38].

## VII. CONCLUSION

In this paper, we applied a perturbative technique to the description of slope selection on a 1D mound in the presence of DF and a large ES barrier. For this purpose, we studied analytically and numerically the solution of systems of ODEs for the terrace widths,  $L_n(t)$ , of 1D step trains, without and with step-step interactions. From a dynamical systems point of view, these ODEs are “nearly recursive,” in the sense that

the contribution to  $dL_n/dt$  from  $L_m$  for  $m > n$  scales with a small parameter,  $\varepsilon_s$ , which expresses the strength of DF relative to the ES barrier.

We applied the perturbative technique to a model for mound slope selection with kinetic parameters derived from a simplified step flow model of constant probabilities for the motion of adatoms on terraces of a semi-infinite system, and from a more complicated step flow model in which the corresponding probabilities depend on terrace widths. In the former model, we analytically derived, directly from the dynamics, the long-time slope of the mound far from its base. In the latter model, we carried out a similar calculation with the help of numerics for finite mounds. A noteworthy result is the characterization of the above simplified model as a plausible *effective theory* of slope selection. The perturbative method is also applicable to other models, including models for 1D mounds with interacting steps or 2D, axisymmetric mounds.

Our analysis leaves some unresolved questions though. The main missing piece of the picture is an understanding of the full dynamical behavior. Specifically, we lack a reliable description of the step annihilation times for desirable initial conditions. If the annihilation times could be computed or at least asymptotically estimated, then the step flow model could be consistently replaced by a continuum theory: an evolution PDE for the height or step density profile along with a step annihilation boundary condition. We hope that our analysis will motivate further studies in this direction.

## ACKNOWLEDGMENTS

The authors wish to thank Prof. J. W. Evans for valuable conversations on slope selection, and Prof. J. P. Schneider for useful discussions on past works in this subject. The research of I.J. and D.M. was supported by NSF Grant No. DMS-1412769 at the University of Maryland. The research of C.R. was supported by NSF Grant No. DMS-1412392 at the University of California, Los Angeles. The research of F.G. was supported by NSF Grant No. DMS-1412695 at the University of California, Santa Barbara.

## APPENDIX: DIRECT ITERATIVE SCHEME FOR SIMPLIFIED STEP FLOW MODEL

In this Appendix, we review the perturbative technique that underlies the computation of the saturation profile within the simplified model of Sec. III. This method makes use of a direct recursive scheme, which exploits the triangular structure of the governing ODE system. By recourse to Sec. III, the starting point is to treat the probability parameter  $P_-$  as small.

In this vein, consider the formal expansion

$$L_n(t) = \sum_{k=0}^{\infty} P_-^k L_n^{(k)}(t), \quad n \geq 0. \quad (\text{A1})$$

Equations (16) indicate that the terrace widths,  $L_n$ , scale proportionally to  $P_+$ . Thus, we define

$$R_n(t) = \frac{L_n(t)}{P_+}.$$

By Eq. (A1), this  $R_n$  is expanded into a series of the form

$$R_n(t) = \sum_{k=0}^{\infty} P_n^k R_n^{(k)}(t).$$

The substitution of  $L_n(t) = P_+ R_n(t)$  by the above formal expansion into Eqs. (16) leads to the following hierarchy for the associated coefficients,  $R_n^{(k)}$ :

$$\frac{dR_0^{(0)}}{dt} = -R_0^{(0)} - 1, \quad (\text{A2a})$$

$$\frac{dR_1^{(0)}}{dt} = R_0^{(0)} - R_1^{(0)} + 1, \quad (\text{A2b})$$

$$\frac{dR_n^{(0)}}{dt} = R_{n-1}^{(0)} - R_n^{(0)}, \quad (\text{A2c})$$

$$\frac{dR_0^{(k)}}{dt} = -R_0^{(k)} - R_1^{(k-1)}, \quad (\text{A2d})$$

$$\frac{dR_1^{(k)}}{dt} = R_0^{(k)} - R_1^{(k)} - R_2^{(k-1)} + 2R_1^{(k-1)}, \quad (\text{A2e})$$

$$\frac{dR_n^{(k)}}{dt} = R_{n-1}^{(k)} - R_n^{(k)} - R_{n-1}^{(k-1)} + 2R_n^{(k-1)} - R_{n+1}^{(k-1)}; \quad n \geq 2, k \geq 1. \quad (\text{A2f})$$

Note that this system exhibits a triangular structure: to compute  $R_n^{(k)}$ , it is necessary to first compute  $R_m^{(k-j)}$  for  $j = 0, 1, \dots$  and  $m = 0, 1, \dots, n+j$ .

The equations of motion for  $R_n^{(k)}$  are supplemented with the terminal conditions

$$L_0(1) = 0, \quad L_n(1) = L_{n-1}(0), \quad n \geq 1.$$

These conditions form the requirements for the saturation profile, discussed in the main text; for example, see Eq. (19). We impose these conditions for the whole hierarchy via

$$R_0^{(k)}(1) = 0, \quad k \geq 0, \quad (\text{A3a})$$

$$R_n^{(k)}(1) = R_{n-1}^{(k)}(0), \quad n \geq 1, \quad k \geq 0. \quad (\text{A3b})$$

We now integrate Eqs. (A2), imposing conditions (A3) as initial conditions. The resulting formulas for  $R_n^{(k)}(t)$  read

$$R_0^{(0)}(t) = e^{1-t} - 1, \quad (\text{A4a})$$

$$R_1^{(0)}(t) = e^{-t} \left\{ eR_0^{(0)}(0) + \int_1^t e^s [R_0^{(0)}(s) + 1] ds \right\}, \quad (\text{A4b})$$

$$R_n^{(0)}(t) = e^{-t} \left\{ eR_{n-1}^{(0)}(0) + \int_1^t e^s [R_{n-1}^{(0)}(s)] ds \right\}, \quad (\text{A4c})$$

$$R_0^{(k)}(t) = -e^{-t} \int_1^t e^s R_1^{(k-1)}(s) ds, \quad k > 0, \quad (\text{A4d})$$

$$R_1^{(k)}(t) = e^{-t} \left\{ eR_0^{(k)}(0) + \int_1^t e^s [R_0^{(k)}(s) - R_2^{(k-1)}(s) + 2R_1^{(k-1)}(s)] ds \right\}, \quad k > 0, \quad (\text{A4e})$$

$$R_n^{(k)}(t) = e^{-t} \left\{ eR_{n-1}^{(k)}(0) + \int_1^t e^s [R_{n-1}^{(k)}(s) - R_{n-1}^{(k-1)}(s) + 2R_n^{(k-1)}(s) - R_{n+1}^{(k-1)}(s)] ds \right\}; \quad n > 1, \quad k > 0. \quad (\text{A4f})$$

The coefficients,  $L_n^{(k)}$ , of expansion (A1) are

$$L_n^{(0)}(t) = R_n^{(0)}(t),$$

$$L_n^{(k)}(t) = R_n^{(k)}(t) - R_n^{(k-1)}(t), \quad k \geq 1.$$

Evidently, hierarchy (A4) may be integrated directly. The key observation is that  $R_n^{(k)}(t) = e^{-t} p_n^{(k)}(t)$  where  $p_n^{(k)}(t)$  is a polynomial of degree at most  $n + 2k$ , except when  $n = k = 0$ . Thus, if we define

$$p_n^{(k)}(t) = \sum_{p=0}^{n+2k} c_{n,p}^{(k)} t^p,$$

the problem reduces to evaluating the requisite coefficients,  $c_{n,p}^{(k)}$ .

We proceed to outline the procedure of determining  $c_{n,p}^{(k)}$ . For  $k = 0$ , we compute

$$c_{1,0}^{(0)} = e(e - 2), \quad (\text{A5a})$$

$$c_{1,1}^{(0)} = e. \quad (\text{A5b})$$

These values serve as initial conditions for the following recursion, with  $n \geq 2$ :

$$c_{n,0}^{(0)} = (e - 1)c_{n-1,0}^{(0)} - \sum_{p=1}^{n-1} \frac{c_{n-1,p}^{(0)}}{p+1}, \quad (\text{A6a})$$

$$c_{n,p}^{(0)} = \frac{c_{n-1,p-1}^{(0)}}{p}, \quad 1 \leq p \leq n. \quad (\text{A6b})$$

The use of Eqs. (A5b) and (A6b) gives

$$c_{n,n}^{(0)} = \frac{e}{n!}, \quad (\text{A7a})$$

$$c_{n,p}^{(0)} = \frac{c_{n-p,0}^{(0)}}{p!}, \quad p < n. \quad (\text{A7b})$$

Putting the pieces of this framework together yields the following recursion relation:

$$c_{n,p}^{(0)} = \frac{1}{p!} \left( (e - 1)c_{n-p-1,0}^{(0)} - \frac{e}{(n-p)!} - \sum_{p'=1}^{n-p-2} \frac{c_{n-p-(p'+1),0}^{(0)}}{(p'+1)!} \right)$$

for  $n \geq 2, p < n$ . Thus, the problem of determining  $c_{n,p}$  is entirely reduced to the case with  $p = 0$ , whose recursion takes the convenient form

$$c_{n,0}^{(0)} = (e - 1)c_{n-1,0}^{(0)} - \frac{e}{n!} - \sum_{p'=2}^{n-2} \frac{c_{n-p',0}^{(0)}}{p'!}$$

for  $n \geq 2$ , initialized by (A5a). The result for the saturation profile to this order is  $\lim_{n \rightarrow \infty} c_{n,0}^{(0)} = 2$ .

The structure of the difference scheme is the same for all orders,  $k > 0$ . The procedure is essentially the same for all orders, but the computation becomes increasingly cumbersome with  $k$ . By using a similar methodology, to the next order,  $k = 1$ , we find the following relations:

$$c_{0,0}^{(0)} = c_{1,0}^{(0)} + c_{1,1}^{(0)} = e(e-1),$$

$$c_{0,p}^{(1)} = -\frac{c_{1,p-1}^{(1)}}{p}, \quad p = 1, 2,$$

$$c_{1,0}^{(1)} = (e-1)c_{0,0}^{(1)} + \sum_{p=0}^2 \frac{c_{2,0}^{(0)}}{p+1} - 2 \sum_{p=0}^1 \frac{c_{1,p}^{(0)}}{p+1},$$

$$c_{1,p}^{(1)} = \frac{c_{0,p-1}^{(1)} - c_{2,p-1}^{(0)} + 2c_{1,p-1}^{(0)}}{p}, \quad p = 1, 2, 3,$$

$$c_{n,0}^{(1)} = (e-1)c_{n-1,0}^{(1)} - \sum_{p=1}^{n+1} \frac{c_{n-1,p}^{(1)}}{p+1} + \sum_{p=0}^{n-1} \frac{c_{n-1,p}^{(0)}}{p+1} - 2 \sum_{p=0}^n \frac{c_{n,p}^{(0)}}{p+1} + \sum_{p=0}^{n+1} \frac{c_{n+1,p}^{(0)}}{p+1}, \quad n \geq 2,$$

$$c_{n,p}^{(1)} = \frac{c_{n-1,p-1}^{(1)} - c_{n-1,p-1}^{(0)} + 2c_{n,p-1}^{(0)} - c_{n+1,p-1}^{(0)}}{p}, \quad n \geq 2, \quad p = 1, 2, \dots, n,$$

$$c_{n,n+1}^{(1)} = \frac{c_{n-1,n}^{(1)} + 2c_{n,n}^{(0)} - c_{n+1,n}^{(0)}}{n+1}, \quad n \geq 2,$$

$$c_{n,n+2}^{(1)} = \frac{c_{n-1,n+1}^{(1)} - c_{n+1,n+1}^{(0)}}{n+2}, \quad n \geq 2.$$

- [1] J. Krug and T. Michely, *Islands, Mounds, and Atoms: Patterns and Processes in Crystal Growth Far from Equilibrium* (Springer, Berlin, 2004).
- [2] A. Pimpinelli and J. Villain, *Physics of Crystal Growth* (Cambridge University Press, Cambridge, 1998).
- [3] H.-C. Jeong and E. D. Williams, *Surf. Sci. Rep.* **34**, 171 (1999).
- [4] C. Misbah, O. Pierre-Louis, and Y. Saito, *Rev. Mod. Phys.* **82**, 981 (2010).
- [5] M. Ozdemir and A. Zangwill, *Phys. Rev. B* **42**, 5013 (1990).
- [6] A. Rettori and J. Villain, *J. Phys. (France)* **49**, 257 (1988).
- [7] D. Margetis and R. V. Kohn, *Multiscale Model. Simul.* **5**, 729 (2006).
- [8] G. Ehrlich and F. G. Hudda, *J. Chem. Phys.* **44**, 1039 (1966).
- [9] R. L. Schwoebel and E. J. Shipsey, *J. Appl. Phys.* **37**, 3682 (1966).
- [10] J. W. Evans, D. E. Sanders, P. A. Thiel, and A. E. DePristo, *Phys. Rev. B* **41**, 5410(R) (1990).
- [11] P. Šmilauer, M. R. Wilby, and D. D. Vvedensky, *Phys. Rev. B* **47**, 4119(R) (1993).
- [12] K. J. Caspersen and J. W. Evans, *Phys. Rev. B* **64**, 075401 (2001).
- [13] S. Schinzer, S. Köhler, and G. Reents, *Eur. Phys. J. B* **15**, 161 (2000).
- [14] M. Li and J. W. Evans, *Phys. Rev. B* **73**, 125434 (2006).
- [15] M. Li and J. W. Evans, *Phys. Rev. Lett.* **95**, 256101 (2005).
- [16] M. Li and J. W. Evans, *Phys. Rev. Lett.* **96**, 079902(E) (2006).
- [17] J. Tersoff, Y. H. Phang, Z. Zhang, and M. G. Lagally, *Phys. Rev. Lett.* **75**, 2730 (1995).
- [18] P. J. H. Bloemen, M. T. Johnson, M. T. H. van de Vorst, R. Coehoorn, J. J. de Vries, R. Jungblut, J. aan de Stegge, A. Reinders, and W. J. M. de Jonge, *Phys. Rev. Lett.* **72**, 764 (1994).
- [19] H.-J. Ernst, F. Fabre, R. Folkerts, and J. Lapujoulade, *J. Vacuum Sci. Technol. A* **12**, 1809 (1994).
- [20] M. Bott, T. Michely, and G. Comsa, *Surf. Sci.* **272**, 161 (1992).
- [21] V. B. Shenoy, S. Zhang, and W. F. Saam, *Phys. Rev. Lett.* **81**, 3475 (1998).
- [22] V. Shenoy, S. Zhang, and W. Saam, *Surf. Sci.* **467**, 58 (2000).
- [23] J. W. Evans, P. A. Thiel, and M. Li, in *Perspectives on Inorganic, Organic, and Biological Crystal Growth: From Fundamentals to Applications: Based on the lectures presented at the 13th International Summer School on Crystal Growth*, edited by M. Skowronski, J. J. DeYoreo, and C. A. Wang, AIP Conf. Proc. No. 916 (AIP, New York, 2007), p. 191.
- [24] J. W. Evans, *Phys. Rev. B* **43**, 3897 (1991).
- [25] J. Schneider, D. Margetis, F. Gibou, and C. Ratsch, *J. Phys.: Condens. Matter* **31**, 365301 (2019).
- [26] M. Siegert and M. Plischke, *Phys. Rev. Lett.* **68**, 2035 (1992).
- [27] M. D. Johnson, C. Orme, A. W. Hunt, D. Graff, J. Sudijono, L. M. Sander, and B. G. Orr, *Phys. Rev. Lett.* **72**, 116 (1994).
- [28] J. A. Stroschio, D. T. Pierce, M. D. Stiles, A. Zangwill, and L. M. Sander, *Phys. Rev. Lett.* **75**, 4246 (1995).
- [29] D. Moldovan and L. Golubovic, *Phys. Rev. E* **61**, 6190 (2000).
- [30] P. Politi and C. Misbah, *Phys. Rev. Lett.* **92**, 090601 (2004).
- [31] P. Politi and C. Misbah, *Phys. Rev. E* **73**, 036133 (2006).
- [32] W. K. Burton, N. Cabrera, and F. C. Frank, *Philos. Trans. R. Soc. London A* **243**, 299 (1951).
- [33] V. I. Marchenko and A. Ya. Parshin, *Sov. Phys. JETP* **52**, 129 (1980).
- [34] R. Najafabadi and D. J. Srolovitz, *Surf. Sci.* **317**, 221 (1994).
- [35] P. Politi and A. Torcini, *J. Phys. A* **33**, L77 (2000).
- [36] A. A. Chernov, *Sov. Phys. Usp.* **4**, 116 (1961).
- [37] M. Ozdemir and A. Zangwill, *Phys. Rev. B* **45**, 3718 (1992).
- [38] P. Politi, G. Grenet, A. Marty, A. Ponchet, and J. Villain, *Phys. Rep.* **324**, 271 (2000).
- [39] P. Politi, *C. R. Phys.* **7**, 272 (2006).
- [40] M. Li, Y. Han, P. A. Thiel, and J. W. Evans, *J. Phys.: Condens. Matter* **21**, 084216 (2009).
- [41] N. Israeli and D. Kandel, *Phys. Rev. B* **60**, 5946 (1999).
- [42] D. Margetis, P.-W. Fok, M. J. Aziz, and H. A. Stone, *Phys. Rev. Lett.* **97**, 096102 (2006).
- [43] S. H. Strogatz, *Nonlinear Dynamics and Chaos with Applications to Physics, Biology, Chemistry, and Engineering* (Westview Press, Boulder, CO, 2015).